University of Texas Rio Grande Valley

ScholarWorks @ UTRGV

Manufacturing & Industrial Engineering Faculty Publications and Presentations

College of Engineering and Computer Science

6-26-2021

A State-of-the-Art Review of Laser-Assisted Bioprinting and its Future Research Trends

Chaoran Dou

Victoria Perez

Jie Qu

Andrew Tsin

Ben Xu

See next page for additional authors

Follow this and additional works at: https://scholarworks.utrgv.edu/mie_fac

 Part of the Industrial Engineering Commons, and the Manufacturing Commons

Authors

Chaoran Dou, Victoria Perez, Jie Qu, Andrew Tsin, Ben Xu, and Jianzhi Li

Check for updates

A state-of-the-art review of Laser-Assisted Bioprinting (LAB) and its future research trends

Chaoran Dou[1], Victoria Perez[1], Jie Qu[2, 3], Andrew Tsin[4], Ben Xu*[5], Jianzhi Li*[1]

[1] Department of Manufacturing and Industrial Engineering, The University of Texas Rio Grande Valley, Edinburg, TX, USA

[2] Department of Mechanical Engineering, The University of Texas Rio Grande Valley, Edinburg, TX, USA

[3] School of Electrical and Power Engineering, China University of Mining and Technology, Xuzhou, Jiangsu, China

[4] Department of Molecular Science, The University of Texas Rio Grande Valley School of Medicine, Edinburg, TX, USA

[5] Department of Mechanical Engineering, Mississippi State University, Starkville, MS, USA

Corresponding Author

Dr. Ben Xu, TEL.: (662) 325-5632; Email: xu@me.msstate.edu

Dr. Jianzhi Li, TEL.: (956) 665-7329; E-mail: jianzhi.li@utrgv.edu

Abstract

Bioprinting is an additive manufacturing technology with great potential in medical applications. Among available bioprinting techniques, laser assisted bioprinting (LAB) is a promising technique due to its high resolution, high cell viability, and the capability to deposit high viscous bioink. These characteristics allow the LAB technology to control cells precisely to reconstruct living organs. This paper is intended to review the recent developments of LAB technologies. It covers various designs of LAB printers, the research progresses in energy absorbing layer (EAL), the physical phenomenon that triggers the printing process in terms of bubble formation and jet development, the printing process parameters, and the major factors related to the post-printing cell viability. This paper highlights the latest studies on LAB technologies, expounds their advantages and disadvantages, and further presents some potential applications. This paper also provides discussions about the potential technical challenges and future research trends for LAB technologies.

Keywords: Bioprinting; Laser assisted bioprinting (LAB); Laser-Induced-Forward-Transfer (LIFT); Regenerative medicine; Additive manufacturing

This is the author manuscript accepted for publication and has undergone full peer review but has not been through the copyediting, typesetting, pagination and proofreading process, which may lead to differences between this version and the Version of Record.
Please cite this article as doi: 10.1002/cben.202000037

This article is protected by copyright. All rights reserved.

Author Manuscript

21969744, 2021, 5, Downloaded from https://onlinelibrary.wiley.com/doi/10.1002/cben.202000037 by The University Of Texas Rio Grande Valley, Wiley Online Library on [13/12/2022]. See the Terms and Conditions (https://onlinelibrary.wiley.com/terms-and-conditions) on Wiley Online Library for rules of use; OA articles are governed by the applicable Creative Commons License

1. Introduction

Bioprinting is a new research area that calls upon knowledge of biology, medical science, material science and manufacturing/mechanical engineering. It has attracted vast interests during the past decade, due to its significant potentials in various biomedical applications [1]. Based on the same principle of additive manufacturing process, it can create complex 3D biostructure by depositing bioink on target substrate or scaffold. The great potential of bioprinting ensures its wide prospects in bio-manufacturing, especially in regenerative medicine and drug development [2].

The primary long-term goal of bioprinting research is to construct functional organs or tissues which can be transplanted [3-5]. For natural tissues or organs in vivo, cells are growing three-dimensionally and communicating spatially. In the past, limited by existing technologies, most cells or tissues are cultured in 2D structures. The lack of a 3D structure may cause cells to lose part of their biological functions because of the limited cell interaction, which eventually leads to difficulties in cell migration, reproduction, and assembly required in tissue regeneration[6-8]. To address this issue, different technologies have been developed to construct 3D biological models. These technologies include the rotating method [9], hanging drop method [10], forced-floating method [11, 12], microfluidic system [13], the use of scaffold [14, 15] and 3D bioprinting [16]. Among all technologies, 3D bioprinting has been proved to be the most promising one to fabricate 3D biological structures with biomaterials, which already shows great potentials in the manufacturing of functional biological tissues even in its infancy [17]. There are four major bioprinting technologies: droplet based bioprinting (DBB), extrusion based bioprinting (EBB), vat polymerization (VP), and laser assisted bioprinting (LAB). While all printing principles find their applications in tissue regeneration, this paper will focus on LAB due to its special design, great potentials and unique technical challenges.

Among all LAB technologies, laser induced forward transfer (LIFT), which is firstly proposed by Bohandy *et al.* in 1986 [18] as an accurate metal deposit technology, has been applied to bioprinting in 2004 for the first time and successfully prints cell patterns with high cell viability [19-21]. LAB has many unique advantages, such as 1) it can deposit material with a higher printing accuracy and resolution than nozzle-based bioprinting. With the appropriate parameters, the printing resolution of LAB can reach up to micron level [22, 23], which provides LAB the capability of isolating single cell or cell aggregations from high cell concentration bioink [24]; 2) equipped with a high frequency pulse laser, LAB can achieve high throughput printing up to 5 kHz, which can translate to 5000 droplets deposited on the substrate per second [22, 25]; 3) Compared to other droplet-based and extrusion-based bioprinting methods, LAB deposits bioink by laser without utilizing any nozzle, which is, however, generally required in other bioprinting processes. This ensures the LAB processing bioink without clogging issue even if the bioink is very viscous [26, 27]. The viscosity range of the bioink that can be handled by the LAB is in the range of 1-8000 mPa·s [2, 28]; 4) Some research groups [29] reported that the LAB can print cells into a high cell density structure. The high cell density is the key feature to ensure the endothelial cells to form the capillary system which is one of the essential research topics in biomanufacturing engineering/science; 5) among all bioprinting technologies, LAB has the highest cell viability; 6) the LAB also has the capability to achieve *in situ* printing [30]. It has been reported that the "multipotent mouse bone marrow stromal precursor cells" was printed on a skull of a mouse to help the recovery of its bone injury [31]; 7) LAB can cooperate with other bioprinting technologies to extend its capability, for example, Ovsianikov *et al.* [32]

This article is protected by copyright. All rights reserved.

Author Manuscript

21969744, 2021, 5, Downloaded from https://onlinelibrary.wiley.com/doi/10.1002/cben.202000037 by The University Of Texas Rio Grande Valley, Wiley Online Library on [13/12/2022]. See the Terms and Conditions (https://onlinelibrary.wiley.com/terms-and-conditions) on Wiley Online Library for rules of use; OA articles are governed by the applicable Creative Commons License

integrated LIFT with the two-photon polymerization technique, which was used to print the scaffold, while LIFT was then used to deposit the cells.

In terms of various types of tissues that can be used in LIFT, it has already been proven that the LIFT bioprinting can process Liposomes [33], DNA [21, 34-37], Proteins [38], human osteosarcoma cells [20], human osteoprogenitor cells [39], human endothelial cells [40], tissue engineered skin substitutes [41, 42], fungi [43], mesenchymal stem cells [44, 45], and human colon cancer cells [46], as shown in Table. 1.

Table.1 Biomaterials processed by LAB

Material	Reference
DNA	[21, 34-37]
Human colon cancer cells	[46]
Human endothelial cells	[40]
Human osteosarcoma cells	[20]
Human osteoprogenitor cells	[39]
Liposomes	[33]
Mesenchymal stem cells	[44, 45]
Proteins	[38]

Even though LAB is one of the most promising bioprinting technologies, it also has some weaknesses that cannot be ignored at the current stage. Limited by the small amount of biomaterials that can be transferred in each laser pulse, the productivity of LAB is not yet the highest among all bioprinting methods. Even equipped with a high frequency laser, the productivity of LAB still cannot compete with other bioprinting methods, such as the inkjet bioprinting, which is a droplet-based bioprinting technology. This could be a significant drawback for medical applications, such as organ printing [47], where the printing speed is a crucial factor in the manufacturing process. The high cost to build a LAB printer is another factor that limits the research and its commercialization.

In order to have a complete understanding of the LAB technologies, we aim to provide a state-of-the-art review about the LAB setup, research gaps, technical challenges and future research trends. This review is organized as follows: Section 2 provides an overview of general LAB setup and its working principle; Section 3 outlines the importance of absorbing layer in details; Section 4 discusses how the printing parameters can affect the printing process; Section 5 introduces a special application of LAB, which is single cell isolation; Section 6 emphasizes the effects of bubble/jet formation on the bioink transfer process; Section 7 mainly lists out all the factors which are essential to the viability of printed cells during or after the printing process. In the end, we also provide some insights about the technical challenges and discuss some future research trends in Bio3D printing.

2. LAB setup and its main modules

The common design and setup of LAB is shown in Fig. 1. It consists of three main modules, the laser generator, the laser path adjusting module, and the cell transfer module. These three main modules work together to deposit the bioink in the desired place. Since the laser path adjusting module simply consists of mirrors and

This article is protected by copyright. All rights reserved.

Author Manuscript

21969744, 2021, 5, Downloaded from https://onlinelibrary.wiley.com/doi/10.1002/cben.202000037 by The University Of Texas Rio Grande Valley, Wiley Online Library on [13/12/2022]. See the Terms and Conditions (https://onlinelibrary.wiley.com/terms-and-conditions) on Wiley Online Library for rules of use; OA articles are governed by the applicable Creative Commons License

lenses to reflect or expand the laser beam, in the following two subsections, only the laser generator and the cell transfer module will be discussed in detail.

Fig. 1 The structure and main components of laser assisted bioprinter (modified from [48])

2.1 Laser generator

Since the invention of LAB, various types of laser generators have been tested for LAB, such as the excimer laser [49], Nd: YVO4 laser [50], Nd:YAG laser[29, 31, 51-53], and ruby laser [54]. The laser wavelength varies from 94nm [54], 266nm [55], 284nm [56], 355nm [51, 53] to 1064nm [31, 52]. In terms of the laser pulse duration, most LAB systems are using nanosecond laser, but the sub-picosecond laser [35, 57], and femtosecond laser [58, 59] have also been tested.

The most commonly used laser pulse duration in the LIFT bioprinting is the nanosecond pulse, however, the heat effect of nanosecond laser becomes a major factor that can cause damages to heat-sensitive cells in the printing process [60]. It is believed that a laser with a shorter pulse duration, such as the femtosecond and picosecond laser, could reduce the heat released to the bioink, thus resolving the problem of thermal damage to cells being printed. Among various laser wavelengths, the infrared laser is preferred, because its wavelength generally causes less change in the chemical and physical properties of the bioink and also creates less damage to cells than the UV laser [25, 61, 62], which is not a good choice when processing living cells because it has the potential risks of breaking the DNA double strand [63]. However, it is worth noting that the laser wavelength also plays an important role in the thermal effect, for example, even though the infrared laser is preferred over the UV laser, it may cause more thermal damages to cells. It is essential to evaluate the influences of pulse duration together with the laser wavelength in order to identify the most appropriate laser for better cell viability.

2.2 Cell transfer module

In a common LIFT setup, the cell transfer module consists of a ribbon and a substrate, which are usually in the shapes of a disk and made of transparent materials such as glass or quartz. The ribbon is set above the substrate with a very small distance, usually 100-500 micron, as shown in Fig. 1. There are two different ribbon setups: 1) matrix assisted pulse laser evaporation direct writing (MAPLE-DW); 2) absorbing layer assisted LIFT (AFA-LIFT). The difference between AFA-LIFT and the MAPLE-DW is with or without an energy absorbing layer. The ribbon in an AFA-LIFT setup has three layers of materials: 1) the supporting structure, which is a relatively thick and transparent layer made of quartz or glass; 2) beneath the first layer, a very thin and nano-scale laser absorbing layer (or sacrifice layer) is coated; 3) the bottom of the whole ribbon setup is named the bioink layer which contains the material that needs to be transferred [64]. But the ribbon structure for MAPLE-DW only has two layers: the supporting layer and the bioink layer [65]. In the MAPLE-DW, due to the no-EAL design, the protein in the bioink is the most widely used laser absorbing matrix, consequently, the low energy UV laser is applied in MAPLE-DW, which is not good for cell viability [63]. The potential method to solve this problem is discussed in Section 3.

On the hard surface of the substrate, some researchers applied a thin layer of “soft buffer” in order to reduce the impact of landing, more information can be found in Section 7.1.

This article is protected by copyright. All rights reserved.

Author Manuscript

21969744, 2021, 5, Downloaded from https://onlinelibrary.wiley.com/doi/10.1002/cben.202000037 by The University Of Texas Rio Grande Valley, Wiley Online Library on [13/12/2022]. See the Terms and Conditions (https://onlinelibrary.wiley.com/terms-and-conditions) on Wiley Online Library for rules of use; OA articles are governed by the applicable Creative Commons License

2.3 Working process

As showed in Fig.2, the working process of LAB is composed of several sequenced steps [51, 66-70]:

1) the laser beam is emitted from the laser generator and the mirrors/lenses adjust the laser path to ensure the laser reaches and focuses on the up surface of the sacrifice layer (in AFA-LIFT) or bioink layer (in MAPLE-DW) after the beam passes through the transparent supporting structure;

2) a bubble is generated and grows at the irradiation spot. The bioink in this area starts to stream along the vacuolar membrane and meet at the bubble pole;

3) the violent expansion of the bubble decreases the inner pressure quickly and the bubble starts to collapse. Driven by the high pressure generated at bubble pole, the bioink forms a jet or droplet;

4) the jet or droplet is then landed on the receiving substrate after traveling through the gap between the ribbon and substrate and a small amount of bioink is deposited on the substrate. The cells or other biomaterial in the bioink is printed.

By repeating these four steps, printing through different areas, droplet by droplet, layer by layer, the designed biological structure will finally be built.

Fig. 2 LAB working process: (a) step 1; (b) step 2; (c) step 3 and (d) step 4

2.4 laser induced backward transfer (LIBT)

Fig. 3 Laser induced backward transfer [58]

There are two potential technical challenges of LIFT technique: 1) the uniformity and stability of the bioink layer cannot be achieved easily with the required low thickness of the bioink layer; 2) the surface tension and evaporation may cause the bioink layer malfunction. The bioink layer is very thin, the surface tension may cause bioink layer to become ununiform and the evaporation may dry up the thin layer very quickly. To resolve these two problems, Duocastella *et al.* [58, 71] proposed a new technique, which is called “laser induced backward transfer (LIBT)” or “film-free laser forward printing”, to address the two aforementioned technical issues of the current LIFT setup. Duocastella *et al.* switched the position of the substrate and bioink donor, the laser beam now goes through the transparent substrate or direct comes from below and focuses at a small distance below the surface of the bioink where the bubble is generated, as shown in Fig. 3. In this method, no EAL is required and the cavitation bubbles are generated by femtosecond infrared laser to propel a small amount of liquid squirting upwards and deposit it on the lower surface of the substrate.

3. Laser absorbing layer of a LAB system

The laser absorbing layer (LAL) or energy absorbing layer (EAL) is one of the essential components of the multilayer ribbon system of AFA-LIFT. It is the base material of bubble formation and provides the ability to absorb the laser energy efficiently and further generate bubble/jet due to evaporation or other mechanisms, which is discussed in detail in Section-6. Generally, the use of EAL in AFA-LIFT can improve the linear laser

This article is protected by copyright. All rights reserved.

Author Manuscript

21969744, 2021, 5, Downloaded from https://onlinelibrary.wiley.com/doi/10.1002/cben.202000037 by The University Of Texas Rio Grande Valley, Wiley Online Library on [13/12/2022]. See the Terms and Conditions (https://onlinelibrary.wiley.com/terms-and-conditions) on Wiley Online Library for rules of use; OA articles are governed by the applicable Creative Commons License

absorption. However, the "film-free laser forward printing" proposed by Duocastella *et al.* [58, 71], actually avoids the use of non-biological, inorganic absorption layers and the use of UV-lasers by a non-linear multi-photon absorption mechanism, eventually creates an optical breakdown to form a jet. In addition, the presence of an independent absorbing layer is the key difference between AFA-LIFT [43, 72] and MAPLE-DW [65]. The absorbing layer provides three major benefits: 1) improve the laser absorbing rate [60, 73]. Bioink may not be able to perform as a good laser absorbing material, because its major contribution is to provide a good environment for the living cells. Due to the weak laser absorption rate of bioink, the absorbing layer is required to enhance the laser energy absorption; 2) isolate the bioink from direct contact with the laser beam, so the EAL greatly reduces the deterioration of cells in the bioink [73, 74]. It was shown [39] that without an EAL, nearly 99% of the laser energy will pass through the bioink layer, and the cells contained in the bioink have a high chance to be destroyed; 3) The EAL also helps the jet formation in the LIFT process. When compared with the case without EAL, it was observed that the jet becomes significantly milder and smoother for the case with EAL, therefore it gives the laser fluence a wide range of tolerance to generate a stable and controllable jet or droplet [75].

However, there are also two drawbacks of having an absorbing layer. First of all, the laser will break the EAL due to the intense energy absorbed, as shown in Fig. 4 [76]. Since the ribbon will be broken after printing, it must be recoated before the next printing, and this will significantly affect the printing efficiency. Secondly, the fragments of the absorbing layer can contaminate the bioink and damage the living cells [50, 77]. While with short pulse duration and low laser energy, the nanosized debris or some nanoparticles from the broken EAL may be negligible [78]. However, the amount of these nanosized fragments will grow with the increase of laser energy and they are hard to be removed [79]. When these fragments accumulate in the printed bioink, the potential risk of cell deterioration increases.

Fig. 4 The morphologies of EAL(titanium) after LAB, a: pulse energy of 2 μJ, spot size of 45 μm, thickness of 160 nm, b: pulse energy of 2 μJ, spot size of 45 μm, thickness of 100 nm, c: pulse energy of 2 μJ, spot size of 45 μm, thickness of 80 nm, d: pulse energy of 2 μJ, spot size of 45 μm, thickness of 40 nm [76]

A good design of EAL can increase printing resolution, promote productivity and enhance cell viability. Various materials have been tried and tested to fabricate the absorbing layer, which include Ti [80], titanium oxide [55, 81], Au [48], Ag [74], and polyimide [50] as shown in table.2. It is believed that the EAL should be thicker than the laser radiation penetration depth for better protection of bioink [82]. For a typical metal EAL, its thickness is usually in the range of 10-100 nm, and for the polymer absorbing layer, the range of thickness is approximately from 500nm to 1000nm [56, 70, 77].

Table.2 EAL materials

EAL material	Reference
Ag	[74]
Au	[48]
Ti	[80]

This article is protected by copyright. All rights reserved.

Author Manuscript

21969744, 2021, 5, Downloaded from https://onlinelibrary.wiley.com/doi/10.1002/cben.202000037 by The University Of Texas Rio Grande Valley, Wiley Online Library on [13/12/2022]. See the Terms and Conditions (https://onlinelibrary.wiley.com/terms-and-conditions) on Wiley Online Library for rules of use; OA articles are governed by the applicable Creative Commons License

Titanium oxide	[55, 81]
Polyimide	[50]

There are two potential ways to solve the contamination caused by EAL fragments. The first one is to print without an EAL, such as the MAPLE-DW technique. As mentioned before, the UV laser is widely used in the MAPLE-DW. The short wavelength laser, unfortunately, will break the double strand of DNA and cause photochemical crosslinking in the bioink [83]. As a result, cells may suffer from death and carcinogenesis. According to the reviewed literature, the best way to improve the MAPLE-DW is to use water as the energy absorbing medium and femtosecond IR laser as the energy source [63]. The second way to solve this issue is to mitigate the contamination caused by EAL fragments. One of the most promising solutions is to adopt the biodegradable material as the EAL. By doing so, the fragments can be degraded and dissolved automatically. Specifically, gelatin has been tested as the material of EAL [83]. With a higher absorbing rate, the gelatin absorbing layer does not need a high laser fluence to generate the bubble and jet, which allows producing a smaller droplet size with lower jet speed, as shown in Fig. 5. Comparing LIFT with and without EAL, the cell viability can be increased by only 10%, but the DNA damage will be decreased significantly by more than 50% [83].

Fig. 5 (a) Droplet size and (b) jet velocity with/without the gelatin EAL. (*) indicates significant difference between groups [83]

To protect the living cells in the bioink in a better way, metallic-foil-assisted laser cell printing was introduced by Lin & Huang [77]. The uniqueness of this technology is the design of the absorbing layer. Different from a single absorbing layer used in a common LIFT setup, this absorbing layer actually consists of two different layers: 1) a sacrifice and adhesive layer; 2) a metallic foil layer, as shown in Fig. 6. The metallic foil is glued underneath the quartz ribbon by 3M Scotch tape. This new design can produce a higher printing resolution while the droplet size is less sensitive to the laser fluence. The printed cells also showed a higher viability under large laser fluence when compared with MAPLE-DW [77]. The sacrifice and adhesive layer will be vaporized, and the metallic foil stays unbroken, which prevents the bioink from contamination during the entire printing process.

Fig. 6 Metallic foil-assisted laser cell transfer [77]

In a typical LIFT setup, the absorbing layer is only for one-time use because the layer will be burned and partially or totally vaporized. The recoating of the absorbing layer is required after each LIFT process, but it may limit the efficiency of LIFT bioprinting. A typical way to resolve this problem is to develop a reusable absorbing layer that is made of materials that cannot be melt or vaporized. Charipar *et al.* [84] developed several reusable absorbing layers, for example, poly (dimethylsiloxane), PDMS (Polydimethylsiloxane), and ceramic thin film comprised of ITO (indium tin oxide). These absorbing layers have been tested in LIFT by printing liquid and solid materials.

This article is protected by copyright. All rights reserved.

Author Manuscript

21969744, 2021, 5, Downloaded from https://onlinelibrary.wiley.com/doi/10.1002/cben.202000037 by The University Of Texas Rio Grande Valley, Wiley Online Library on [13/12/2022]. See the Terms and Conditions (https://onlinelibrary.wiley.com/terms-and-conditions) on Wiley Online Library for rules of use; OA articles are governed by the applicable Creative Commons License

21969744, 2021, 5, Downloaded from https://onlinelibrary.wiley.com/doi/10.1002/cben.202000037 by The University Of Texas Rio Grande Valley, Wiley Online Library on [13/12/2022]. See the Terms and Conditions (https://onlinelibrary.wiley.com/terms-and-conditions) on Wiley Online Library for rules of use; OA articles are governed by the applicable Creative Commons License

4. Parameters related to printing performance

The performance of LIFT bioprinting highly depends on the printing parameters, which play critical roles in the bubble formation, jet development, deposition volume, resolution, and cell viability. Generally, the important printing parameters [70, 76, 85, 86] include:

1. Laser fluence (which equals laser pulse energy divided by laser spot size)
2. The thickness of the absorbing layer
3. The thickness of the bioink layer
4. Travel distance
5. Physical properties of the bioink

By increasing the laser pulse energy, there are three regimes (subthreshold regime, jetting regime and plume regime) that appeared in the jet formation [25, 67, 87], as shown in Fig. 7. If the laser energy is too low or the liquid viscosity is too high, the jet cannot be developed completely, which may result in no material transfer [88, 89]. When the laser energy is higher than the jetting threshold but lower than the plume threshold, a stable jet will appear and the bioink can be transferred in an organized way. In this range, the volume of deposited biomaterial linearly depends on the laser pulse energy [70]. If the laser energy is too high or the viscosity is too low, the jet becomes unstable and the undesired plume appears underneath the bubble, as shown in Fig. 7 [28]. It is noteworthy that the laser energy is not the only parameter that determines the jet regimes. The viscosity of bioink also plays an important role here. When the bioink viscosity gets higher, it needs more laser energy to trigger the jet formation process. If the bioink viscosity is low, splashing is very likely to occur[90].

Fig. 7 Three regimes for bubble/jet fprmation [70]

It was reported that the volume of deposition has a linear relation with the laser fluence [22, 39, 51, 53, 62, 91], as shown in Fig. 8 and Fig. 9. Higher laser fluence means that more cells can be transferred each time [76]. But Lin *et al.* [26] pointed out that it is not the volume, but the droplet diameter is linearly increasing with the laser energy.

Fig. 8 Droplets transferred at different laser energies (Over each column, the average pulse energy is indicated) [53]

Fig. 9 Droplet volume versus laser pulse energy [53]

A smaller laser spot size will result in a better printing resolution [85], however, it is not always desirable because less material will be transferred every time, which will reduce the printing efficiency. Consequently, it is necessary to balance the printing resolution and printing efficiency. Generally, a higher laser fluence has a better potential to rupture the EAL, for the gold EAL, it has been reported that the quantity of fragments linearly grows with the increasing of laser energy per pulse [78], which is not preferred in the LAB. In this case, larger laser spot size, which means lower laser density at same laser pulse energy, may possess the advantages of generating

This article is protected by copyright. All rights reserved.

Author Manuscript

bubble/jet without producing fragments from EAL [50]. When the distance between the ribbon and the substrate is less than 500 microns, in the experiments performed by Deng *et al.* [76], the jet can not be fully developed before the bioink touches the substrate, the volume of bioink and the number of cells transferred to the substrate cannot be controlled well. Once the distance is greater than the threshold, the number of cells printed everytime becomes stable , in this case, the distance has negligible effects on the number of deposited cells [76].

Viscosity, one of the material properties of bioink, is very important to the printing quality. As discuessed above, printing resolution strongly depends on the laser energy and bioink viscosity [85, 92]. Especially when the laser fluence is low, the resolution is more sensitive to the viscosity than laser fluence, and vice versa. The viscosity of bioink will also affect the spreading of droplets during the landing process. It is reported that the size of the deposited droplet is inversely proportional to the viscosity of bioink [22], which means that with the increase of viscosity, the ability to control the printed structure and the printing resolution increases dramatically[85].

Besides viscosity, the cell itself also plays an important role [93]. The presence of cells may change the printability of bioink significantly. The cell-laden bioink has a higher transfer threshold, lower jet velocity, shorter jet break up length, and smaller printed droplet size. Due to the inhomogeneity caused by the living cells in the bioink, the jet may appear non-ideal morphology, such as a non-straight jet with non-straight trajectory or a straight jet with non-straight trajectory [93], as shown in Fig. 10.

Fig. 10 Different types of jets by using the cell-laden bioink [93]

Up until now, the efforts of optimizing the printing parameters to print cells with higher viability and better quality are still limited to few cell types, such as endothelial cells and colon cancer cells [40, 46, 94]. A general method to assign optimal values to printing parameters for each particular printing task with different cells with various shapes and sizes is still desired to be developed. Jie *et al.* [95] proposed a numerical study to simulate the bubble formation and jet process under a single laser pulse, and their simulation results showed that under a laser pulse with the Gaussian distribution, a vapor bubble was formed around 0.1μs, during the bubble expansion process, the maximum magnitude of velocity could reach as high as 22m/s, and the pressure near the laser interaction area was around 4.72×10^7 Pa, which is 470 times of the ambient pressure. Based on the simulation results, they recommended some printing parameters, such as the laser fluence and the focal spot area, in order to achieve a stable regular jet flow to transfer the bioink to the receiving substrate.

5. Single cell isolation

From the discussions in Section-4 regarding the parameters, it can be concluded that by applying the desired value for each parameter, the printing process can be controlled accurately, providing the LAB process the great potential to realize one of the essential applications in medical research: single cell isolation.

The cell is the elementary unit to build up organs and tissues [96]. The high resolution and great viability are critical for LAB to process cells accurately and also isolate single cell during the printing. Therefore it ensures the feasibility of research on the influence of cell microenvironments, single cell analysis, and other research topics [97-100].

This article is protected by copyright. All rights reserved.

Author Manuscript

21969744, 2021, 5, Downloaded from https://onlinelibrary.wiley.com/doi/10.1002/cben.202000037 by The University Of Texas Rio Grande Valley, Wiley Online Library on [13/12/2022]. See the Terms and Conditions (https://onlinelibrary.wiley.com/terms-and-conditions) on Wiley Online Library for rules of use; OA articles are governed by the applicable Creative Commons License

The inkjet-based bioprinting technique has already been tested to print single cell [101], but it still cannot deposit a cell at a time precisely. It was reported that LAB can transfer a single cell every time if proper printing parameters are applied [24]. However, this so-called single cell printing is based on statistical data such as 25 cells are printed by 25 laser pulse and the process cannot be repeated precisely [76, 102]. In some experiments, beads are used to represent real cells due to their similarity in shape and size. It has been found that the number of beads per printed spot is a game of possibility [103]. As shown in Fig. 11, the number of beads in each spot can vary between 0 and 6, the probability of different number of beads depends on the value of printing parameters. The best result that can be achieved is to make the probability of "one bead per spot" become the highest among all other cases. There is no way to guarantee that one laser pulse can induce a single cell accurately.

Fig. 11 The number of beads printed every time with concentrations of 1.0, 1.3, and 1.9×10^7 beads/ml [103]

Marquez *et al.* [104] demonstrated the capability of a new blister actuated-LIFT (BA-LIFT) configuration for cell-laden hydrogel printing at a wide range of viscosities and droplet sizes, and for live tracking and isolation of single cells. In their experiment, the bioink with a concentration of 8~10×10^6 cells per milliliter was prepared by mixing the cells and hydrogel. The cells were isolated along the whole ribbon surface with high viability. It is noteworthy that the cell in the bioink should have at least 50 μm between each other, otherwise more than one cell will be transferred by laser pulse each time. This requirement implies the cell concentration in the bioink should be kept at a relatively low level in order to maintain such a minimum distance.

Even though LAB is the best among all bioprinting techniques in terms of controlling the number of cells printed each time, it is almost impossible to achieve the same number of cells in each droplet due to the random distribution of cells in the bioink. One of the promising solutions is to locate every target cell before printing. By knowing the exact location of each target cell on the ribbon, the laser can be guided to focus on the center of a cell. Doing so not only can solve the problem caused by the random distribution of cells in the bioink, but also may prevent some non-straight jet shapes caused by the presence of cells, which may affect the printing accuracy [93].

6. Bubble/jet formation

Even though in the past 15 years many different types of lasers and ribbon structures have been tested in LAB system, they all share the similar mechanism for the bioink transfer phenomenon: by absorbing the energy of laser pulse, a bubble with much higher inner pressure than its surroundings is generated at the ribbon-bioink interface may be due to evaporation, cavitation, and plasma formation [105, 106]. Then the material beneath the bubble is propelled by forming a droplet or a jet simultaneously while the bubble itself is developing [68, 69].

Scientists tried to optimize the performance of LIFT by testing out the influence caused by varying different parameters, such as the laser fluence, bioink viscosity, and so on. Overall, it can be concluded that the expansion of bubbles provides the momentum for material transfer; the bubble formation and expansion mode play a key role to achieve a less violent transfer process with a higher viability of target cells. The bubble/jet formation process needs to be managed in order to control the accurate amount of material in the transferring process.

This article is protected by copyright. All rights reserved.

Author Manuscript

21969744, 2021, 5, Downloaded from https://onlinelibrary.wiley.com/doi/10.1002/cben.202000037 by The University Of Texas Rio Grande Valley, Wiley Online Library on [13/12/2022]. See the Terms and Conditions (https://onlinelibrary.wiley.com/terms-and-conditions) on Wiley Online Library for rules of use; OA articles are governed by the applicable Creative Commons License

In the LIFT bioprinting process, the critical step is the transfer of biomaterial from the ribbon to the substrate due to the formation of bubble and jet. Unfortunately, the fundamental mechanism that triggers the formation of bubble or jet in LIFT has not been fully understood [68]. Even though a lot of experimental studies have been reported to visualize the process using high speed camera, the theoretical explanation of the formation of bubble or jet, as well as the interaction between the laser and the bioink, has not been comprehended yet.

It has been proven that the jet formation is highly related to the bubble behavior during its expansion and collapse [25, 50, 62, 68, 87, 107]. To specify the bubble/jet formation in the whole printing process as described in Section 2.3, it is divided into three stages by different inner bubble pressures [50, 68, 107] as shown in Fig. 12 and 13. Firstly, the bubble inner pressure is lower than the surrounding pressure, the bubble expands very rapidly and drives the bioink downwards. Secondly, the inner pressure is gradually released to its surrounding pressure, and then the bubble keeps expanding due to the inertia. When the inside pressure equals to the surrounding pressure, the bubble can have a short time of oscillation [50]. Lastly, once the bubble expands to a level where its pressure is lower than the surrounding pressure but still higher than the local saturated vapor pressure, the bubble will start to shrink and collapse, then the jet can be generated.

Fig. 12 Time-resolved images of the jet formation during LAB. Laser power: (a) 1.6 J/cm^2 and (b) 2.7 J/cm^2 [68]

Fig. 13 The bubble/jet formation process of LAB [68]

To explore the physics of material transfer in the LIFT process, scientists developed many attractive hypotheses to explain the experimental phenomenon, such as the plasma formation model, the nucleate boiling model, the phase explosion model, the shock wave model, and the thermo-elastic effect model [105, 106]. Researchers also claimed that their models can only match well with their own experiments, so a generalized model is required to explain the bubble formation and jet development by considering different operating conditions, in order to obtain a comprehensive understanding of the interaction between the laser and the bioink and/or EAL. In this section, we provide a review of all different hypothesis models, and hopefully, this review can trigger some interdisciplinary ideas in the bioprinting research community in order to fulfill the mission of developing a comprehensive model to tackle the bubble formation and jet development.

The plasma formation model requires a high fluence laser to trigger the optical breakdown of the matrix. Generally, the optical breakdown is a high power-consuming process, and the threshold of an optical breakdown of water is around 10^{10} W/cm^2 for nanosecond lasers [108, 109], and slightly above 3×10^{12} W/cm^2 for 340 fs laser with 1040 nm wavelength [109]. Lin *et al.* [26] used a laser with 193nm wavelength, 12ns pulse duration and 1439+/-89 mJ/cm^2 laser fluence for MAPLE-DW printing. When the laser beam was focused at a spot diameter of 150 μm, the laser energy intensity was at the order of 10^8 W/cm^2; therefore, it was much lower than the optical breakdown threshold for water. Therefore, the absorption of the MAPLE-DW is based on linear absorption by using a nanosecond laser pulse, which can heat the bioink and generate a bubble due to evaporation. However, Duocastella *et al.* [58] reported a different result. In their experiment, a femtosecond laser was used for film-free laser forward printing, and the laser had a 1027nm wavelength, 450fs pulse duration, 2 μJ pulse energy, and laser spot size diameter was around 1.2 micron. According to their calculation, the laser

This article is protected by copyright. All rights reserved.

Author Manuscript

21969744, 2021, 5, Downloaded from https://onlinelibrary.wiley.com/doi/10.1002/cben.202000037 by The University Of Texas Rio Grande Valley, Wiley Online Library on [13/12/2022]. See the Terms and Conditions (https://onlinelibrary.wiley.com/terms-and-conditions) on Wiley Online Library for rules of use; OA articles are governed by the applicable Creative Commons License

intensity was about 10^{14} W/cm^2, which is two-order of magnitude higher than the threshold of plasma formation in water. Therefore, they draw a conclusion that it was the plasma expansion that initiates a cavitation bubble, and later it also provided the required kinetic energy to form a jet. Therefore, Duocastella *et al.* concluded that the film-free laser forward printing avoids the use of non-biological, inorganic absorption layers and the use of UV-lasers by a non-linear multi-photon absorption mechanism, and a focused femtosecond laser was used to create an optical breakdown, resulting in the formation of a cavitation bubble to form a jet.

When the laser pulse duration is shorter than 100ns, the boiling can barely occur in such a short time period [26]. The phase explosion is, therefore, considered as a possible reason for the bubble generation in LIFT and MAPLE-DW using short pulse laser (around 10 ns). After a short time period when the laser is focused on the absorbing matrix, the liquid can be heated up to a temperature much higher than its boiling temperature and then reach an equilibrium state of mixed phases. This process is called the phase explosion. The pressure generated by the phase explosion is usually much higher than it generated by the thermoelastic effect; sometimes it can even reach one order of magnitude larger [26]. A nucleation-based phase explosion model was applied in the simulation performed by Xiong *et al.*[106], and their simulation results matched well with the experiments, as shown in Fig. 14 and 15, both results showed that the bubble diameter increases as the laser fluence increases. However, there is an underestimate of the bubble size in the simulation. There are three possible reasons: 1) the bubbles developed in the experiments were ellipse instead of perfect round shape, and the long axe was measured for the diameter; 2) compare to the simulation, some parameters may have different values in the real conditions, such as the portion of the laser energy that absorbed for the bubble formation and temperature rise, in the simulation performed by Xiong *et al.* [106], which was set to 0.65, should be higher in the real printing condition; 3) the classical nucleation theory adopted in the simulation may not be a perfect fit for the low fluence conditions in the experiments.

Fig. 14 Transferred droplet volume versus laser pulse energy [106]

Fig. 15 Maximum bubble diameter under a 722 mJ/cm2 laser fluence[106]

It is essential to understand the physics of LAB in order to improve its printing accuracy and efficiency in terms of promoting cell viability and adapting different printing patterns. However, the bubble and jet formation is a complex multiphase and multiphysics process; more researches are required in this topic in order to further advance the fundamental understanding of laser-bioink interaction and the LIFT biomaterial transfer process.

7. Viability and proliferation

The ultimate goal of bioprinting is to fabricate transplantable organs and tissues, however, it is difficult to process the cells in the bioink, and to provide a perfect environment to help the cells sustain their morphologies and functions during and after bioprinting [110]. It has been proven by Catros *et al.* [39] that the physico-chemical and crystallographic properties of the bioink will be changed slightly by the laser pulse, no matter how powerful the laser is. Furthermore, every step in the printing process has the risk of damaging cells and affecting their viability and proliferation [111-114]. For example the mechanical damage in the transfer and landing

This article is protected by copyright. All rights reserved.

Author Manuscript

21969744, 2021, 5, Downloaded from https://onlinelibrary.wiley.com/doi/10.1002/cben.202000037 by The University Of Texas Rio Grande Valley, Wiley Online Library on [13/12/2022]. See the Terms and Conditions (https://onlinelibrary.wiley.com/terms-and-conditions) on Wiley Online Library for rules of use; OA articles are governed by the applicable Creative Commons License

process, the laser radiation damage, and the thermal damage before the cell transfer process. Therefore, the viability and proliferation behavior of the printed cells become two of the most essential indexes to evaluate a bioprinting method. From this point of view, the LAB is the best approach among all 3D bioprinting technologies due to its highest cell viability and limited damage brought to transferred cells during the whole printing process [115]. After being printed, the cells usually have viability greater than 80%, some researchers reported the cell viability is greater than 95% or even near 100% [20, 55, 72, 116, 117]. Almost all experiments support the claim that the cells recover and start to proliferate like normal cells after a certain period of time after printing [19, 103, 118].

High viability indicates limited damages caused by the printing process, but it doesn't mean zero cell damage or death. Several experimental results have been reported and concluded a standard of LIFT-based bioprinting: higher laser energy may cause a higher cell death rate because some researchers reported that there is no significant difference in cell viability between low and high laser energy inputs [112], as shown in Fig. 16, therefore, the bioink with higher viscosity provides a better protection than the bioink with lower viscosity [112].

Fig. 16 Effect of laser energy on cell viability (Bar = 100μm) [112]

The causes of cell injury in LAB need to be explored in order to guide the optimization of the printing process, such as the physical deformation caused by acceleration and deceleration during bubble expansion and landing process, the exposure to the extreme laser light, the thermal injury caused by the rapid local temperature change in the bioink, and the chemical change of bioink and lack of nutrients [46, 119].

7.1 Mechanical injury

Among all factors, the mechanical force is the main factor that is responsible for cell damage and death, and the mechanical injury to the cells usually is caused by high velocity and frequent switch between acceleration and deceleration during the bubble/jet formation and landing process. Both the acceleration and deceleration processes cause great pressure (normal stress) on the living cells. In addition, the large shear stress caused by the acceleration and deceleration can also jeopardize the structures of living cells. Therefore, the shear stress cannot be ignored even though it is much smaller in LIFT than it in nozzle-based bioprinting [105]. The cell viability gets worse when the laser fluence increases and causes a higher shear stress on the cells [86]. Larger shear stresses may kill cells by damaging the membrane [83, 120] and breaking the DNA double strand [83, 120]. Furthermore, it can interfere with the direction of stem cells' differentiation [121], which may cause a big issue for LAB.

When the laser radiates on the ribbon, the bubble generates, expands, and transfers a small amount of bioink into a high-speed jet. The highest jet velocity can reach 500-1000 m/s and the acceleration in this process can be as high as 10^5-10^9 g [105, 122]. In an experiment performed by Hopp *et al.* [72], the bioink jet has an acceleration about 10^7g within about 1 microsecond, but the study showed that the cells didn't suffer from serious mechanical damages, so they concluded that the cells used in their experiments (Rat Schwann and astroglial cells and pig lens epithelial cells) may tolerate huge acceleration.

This article is protected by copyright. All rights reserved.

Author Manuscript

21969744, 2021, 5, Downloaded from https://onlinelibrary.wiley.com/doi/10.1002/cben.202000037 by The University Of Texas Rio Grande Valley, Wiley Online Library on [13/12/2022]. See the Terms and Conditions (https://onlinelibrary.wiley.com/terms-and-conditions) on Wiley Online Library for rules of use; OA articles are governed by the applicable Creative Commons License

The deceleration process refers to the landing process, which has two types of impacts if the substrate has been coated with a layer of liquid as a landing buffer [112]: the air-liquid interface impact, and the liquid-solid interface impact. The second impact is considered as a "hard landing" when compared with the first impact of "soft landing". Obviously, the "hard landing" may cause more mechanical injuries because the cells crash into the solid surface. In the experiment conducted by Catros *et al.* [112], some heavily deformed cells were observed near the liquid-solid interface while there were no deformed cells at the air-liquid interface. Coating a thicker "landing buffer" can prevent the cell from damage in the landing process. Printing with the laser energy of 8 μJ per pulse, the cell mortality is around 50% when using the 20 μm "landing buffer", which is greater than the 40 and 100 microns "landing buffer", which are 30% and 10% respectively. Furthermore, almost all the cells (nearly 100%) printed on the 20 μm buffer showed a shrunk morphology. They cannot proliferate and separate on the substrate, which means they can be considered dead. This kind of cell also partially appears in the post-printing observation by using 40 and 60 μm buffer layer but shows no trace in the experiment using 80 and 100 μm buffer layer. Interestingly, the soft landing condition can improve the cell viability; the liquid buffer-coated "soft ribbon" can also provide a "safe" environment by slowing down the jet velocity. Not only the buffer-coated receiving substrate but also the EAL with buffer can enhance the cell viability. By coating an additional hydrogel layer between the Ti EAL and the cell medium, the printed cells enjoy higher viability than the case without such a layer [123].

To protect the living cells from mechanical injury, scientists also utilized the gelation in the bioprinting, usually, they combine alginate and calcium chloride. The gelation can provide a buffer as a soft landing condition, however, it may also create isolation between the cells and the nutrients in the bioink [86]. The gelation time of 2 mins resulted in a higher cell viability than 10 minutes of gelation case when observed 24 hours after the printing. This is probably because a thicker gel prevented the cells from absorbing oxygen and nutrients from the environment. Due to the limited nutrition absorption, the cell group that went through 10 mins gelation process had less recovery ability than the group for 2 mins gelation process.

7.2 Thermal injury

The bioink is heated by the laser at the initial stage of cell transfer when the laser interacts with the EAL or laser absorbing matrix. The laser fluence is so high and focused at a small spot size that could cause thermal injury to cells in the bioink by deactivating the enzymes and denaturing the proteins [124]. Even though the thermal injury can be fatal to cells, there are some papers reported that the thermal injury is negligible when compared to the mechanical injury [46, 52, 76], because in a few nanoseconds, the high temperature can only diffuse through a few microns, which is a relatively small distance when compared with the thickness of the bioink. More researches are required in order to reveal the mystery about the thermal injuries.

7.3 Radiative injury

Exposing to the short wavelength laser, such as the UV laser, with high energy density could be one of the reasons that cause cell injury, because the UV light may damage the DNA double strand and kill the living cells. However, Barron *et al.* [103] stated that the UV light and heat only caused minor damage to the printed cells even in extreme conditions that without EAL, in which condition 99% of the laser energy pass through the

This article is protected by copyright. All rights reserved.

Author Manuscript

21969744, 2021, 5, Downloaded from https://onlinelibrary.wiley.com/doi/10.1002/cben.202000037 by The University Of Texas Rio Grande Valley, Wiley Online Library on [13/12/2022]. See the Terms and Conditions (https://onlinelibrary.wiley.com/terms-and-conditions) on Wiley Online Library for rules of use; OA articles are governed by the applicable Creative Commons License

bioink. The AFA-LIFT is a good choice to further mitigate the radiative injury because the EAL can block most of the radiation before it can contact the cells. Furthermore, their experiment also indicated that even with a very thin Titanium absorbing layer (20 nm), 60% of the laser radiation can be absorbed. The other 40% of the laser radiation went through the EAL, thus a cell damage zoom with only 2 microns depth is created, and therefore only about 7% of the bioink was affected. To sum up, in most cases, the cell damage caused by laser radiation is negligible when compared with mechanical injuries [76].

8. Technical challenges and future research trends

From the discussions above, LAB has many advantages, such as high printing resolution, high throughput, high cell viability and good adaptivity with other bioprinting techniques, but it also has many technical challenges and needs more research developments, as discussed in the following perspectives:

1) The wiedly used viscosity of the bioink is ranging from 1 to 8000 mPa·s, which is still not viscous enough to build a solid structure without any support. A good printing environment that can provide enough support for the printed structure should be developed, such as submerging the substrate into a bioink environment to utilize the bioink as a supporting structure. The other way is to use bioink with high viscosity. The high viscosity will challenge the printability of the bioprinter since it needs more power to transfer the bioink to the substrate. In this case, the EAL will play an important role. New materials should also be explored for better EAL performance. Graphene could be a promising material for two reasons: first, its black color can provide a better laser absorbing rate; second, its biocompatibility may prevent the cells from being contaminated by the EAL fragments.
2) Real organ printing is very different from the experiment performed in the lab since it involves different types of cells with different shapes. One possible solution is to culture the different cells into various modules as in the real in-vivo environment; therefore it can reduce the complexity of printing protocols. For example, the retina is composed of many cells with different shapes, such as rod and cone, but they share the same layer in the retina structure, thus it is extremely challenging to print those cells separately. If the various types of cells can be pre-assembled in the culturing process before the printing, they can be printed as a module instead of different types of cells.
3) Another barrier between laboratory benchtop and factory production is the scaling issue. Limited by the current printing speed, the LAB technology is not able to fabricate bio-product on a large scale, such as interacting synthetic cells and biological communities. In the future, the uncovered fundamental biological principles should seamlessly integrate with biomanufacturing technology to achieve high speed and large scale biofabrication.
4) The physics behind the bubble/jet formation is another essential topic of the LAB. By testing different hypotheses, an accurate physical model should be established in order to precisely predict the initial bubble formation in the printing and the jet development under various printing conditions. In addition, the interaction between laser and bioink with different viscosities is another topic that needs more research attention. The bubble/jet formation process is a violent process with high acceleration, high speed, big pressure, and temperature change. A good study of it can eventually guide the optimization of bioprinting process to achieve higher cell viability, even though LAB already has the best cell survival rate.

This article is protected by copyright. All rights reserved.

Author Manuscript

21969744, 2021, 5, Downloaded from https://onlinelibrary.wiley.com/doi/10.1002/cben.202000037 by The University Of Texas Rio Grande Valley, Wiley Online Library on [13/12/2022]. See the Terms and Conditions (https://onlinelibrary.wiley.com/terms-and-conditions) on Wiley Online Library for rules of use; OA articles are governed by the applicable Creative Commons License

5) Researchers claimed that the fragments of EAL can harm the living cells in the LAB process, however, some researchers announced that some nanoparticles can actually have complex effects on organisms such as microalgae [125]. For another example, the silver nanoparticles can stimulate or stop the proliferation of the cells under different conditions [126, 127]. If the nanofragments from EAL can be utilized, it may have the potential to act as nutrients and further support the living cells during and after the printing.

Acknowledgements

The authors are grateful for the financial support for this work from the US Department of Defense Manufacturing Engineering Education Program (MEEP) (Award number N00014-19-1-2728), the Bose Family Donation to the Department of Manufacturing and Industrial Engineering at UTRGV, and the start-up fund at Mississippi State University.

Abbreviations

AFA-LIFT	Absorbing film-assisted laser induced forward transfer
BA-LIFT	Blister actuated-laser induced forward transfer
DBB	Droplet based bioprinting
EAL	Energy absorbing layer
IR	Infra-red
EBB	Extrusion based bioprinting
LAB	Laser assisted bioprinting
LAL	Laser absorbing layer
LIBT	Laser induced backward transfer
LIFT	Laser induced forward transfer
MAPLE-DW	Matrix-assisted pulse laser evaporation–direct write
UV	Ultraviolet
VP	Vat polymerization

References

[1] C. Mandrycky, Z. Wang, K. Kim, D.H. Kim, *Biotechnol Adv* **2016**, *34(4)*, 422-434. DOI: 10.1016/j.biotechadv.2015.12.011
[2] S.V. Murphy, A. Atala, *Nat Biotechnol* **2014**, *32(8)*, 773-785. DOI: 10.1038/nbt.2958
[3] S.V. Murphy, A. Skardal, A. Atala, *J Biomed Mater Res A* **2013**, *101(1)*, 272-284. DOI: 10.1002/jbm.a.34326
[4] A. Skardal, A. Atala, *Ann Biomed Eng* **2015**, *43(3)*, 730-746. DOI: 10.1007/s10439-014-1207-1
[5] I.T. Ozbolat, Y. Yu, *IEEE Transactions on Biomedical Engineering* **2013**, *60(3)*, 691-699. DOI: 10.1109/TBME.2013.2243912
[6] K.L. Schmeichel, M.J. Bissell, *J Cell Sci* **2003**, *116(Pt 12)*, 2377-2388. DOI: 10.1242/jcs.00503
[7] S. Breslin, L. O'Driscoll, *Drug Discov Today* **2013**, *18(5-6)*, 240-249. DOI: 10.1016/j.drudis.2012.10.003
[8] J.B. Kim, *Semin Cancer Biol* **2005**, *15(5)*, 365-377. DOI: 10.1016/j.semcancer.2005.05.002

This article is protected by copyright. All rights reserved.

Author Manuscript

21969744, 2021, 5, Downloaded from https://onlinelibrary.wiley.com/doi/10.1002/cben.202000037 by The University Of Texas Rio Grande Valley, Wiley Online Library on [13/12/2022]. See the Terms and Conditions (https://onlinelibrary.wiley.com/terms-and-conditions) on Wiley Online Library for rules of use; OA articles are governed by the applicable Creative Commons License

[9] T.J. Goodwin, T.L. Prewett, D.A. Wolf, G.F. Spaulding, *Journal of Cellular Biochemistry* **1993**, *51(3)*, 301-311. DOI: 10.1002/jcb.240510309
[10] J.M. Kelm, N.E. Timmins, C.J. Brown, M. Fussenegger, L.K. Nielsen, *Biotechnology and Bioengineering* **2003**, *83(2)*, 173-180. DOI: 10.1002/bit.10655
[11] A. Ivascu, M. Kubbies, *J Biomol Screen* **2006**, *11(8)*, 922-932. DOI: 10.1177/1087057106292763
[12] R.L.F. Amaral, M. Miranda, P.D. Marcato, K. Swiech, *Front Physiol* **2017**, *8(*605. DOI: 10.3389/fphys.2017.00605
[13] P.J. Lee, N. Ghorashian, T.A. Gaige, P.J. Hung, *JALA Charlottesv Va* **2007**, *12(6)*, 363-367. DOI: 10.1016/j.jala.2007.07.001
[14] E. Sachlos, J.T. Czernuszka, *Eur Cell Mater* **2003**, *5(*29-39; discussion 39-40. DOI: 10.22203/ecm.v005a03
[15] T. Billiet, M. Vandenhaute, J. Schelfhout, S. Van Vlierberghe, P. Dubruel, *Biomaterials* **2012**, *33(26)*, 6020-6041. DOI: 10.1016/j.biomaterials.2012.04.050
[16] S.M. Peltola, F.P. Melchels, D.W. Grijpma, M. Kellomaki, *Ann Med* **2008**, *40(4)*, 268-280. DOI: 10.1080/07853890701881788
[17] Y.S. Zhang, A. Arneri, S. Bersini, S.R. Shin, K. Zhu, Z. Goli-Malekabadi, J. Aleman, C. Colosi, F. Busignani, V. Dell'Erba, C. Bishop, T. Shupe, D. Demarchi, M. Moretti, M. Rasponi, M.R. Dokmeci, A. Atala, A. Khademhosseini, *Biomaterials* **2016**, *110(*45-59. DOI: 10.1016/j.biomaterials.2016.09.003
[18] J. Bohandy, B.F. Kim, F.J. Adrian, *Journal of Applied Physics* **1986**, *60(4)*, 1538-1539. DOI: 10.1063/1.337287
[19] J.A. Barron, P. Wu, H.D. Ladouceur, B.R. Ringeisen, *Biomedical Microdevices* **2004**, *6(2)*, 139-147. DOI: 10.1023/B:BMMD.0000031751.67267.9f
[20] J.A. Barron, B.J. Spargo, B.R. Ringeisen, *Applied Physics A* **2004**, *79(4-6)*, 1027-1030. DOI: 10.1007/s00339-004-2620-3
[21] J.M. Fernández-Pradas, M. Colina, P. Serra, J. Domínguez, J.L. Morenza, *Thin Solid Films* **2004**, *453-454(*27-30. DOI: 10.1016/j.tsf.2003.11.154
[22] B. Guillotin, A. Souquet, S. Catros, M. Duocastella, B. Pippenger, S. Bellance, R. Bareille, M. Remy, L. Bordenave, J. Amedee, F. Guillemot, *Biomaterials* **2010**, *31(28)*, 7250-7256. DOI: 10.1016/j.biomaterials.2010.05.055
[23] V.S. Cheptsov, S.I. Tsypina, N.V. Minaev, V.I. Yusupov, B. Chichkov, *International Journal of Bioprinting* **2018**, *5(1)*. DOI: 10.18063/ijb.v5i1.165
[24] B.R. Ringeisen, S.E. Lizewski, L.A. Fitzgerald, J.C. Biffinger, C.L. Knight, W.J. Crookes-Goodson, P.K. Wu, *Electroanalysis* **2010**, *22(7-8)*, 875-882. DOI: 10.1002/elan.200880012
[25] F. Guillemot, A. Souquet, S. Catros, B. Guillotin, J. Lopez, M. Faucon, B. Pippenger, R. Bareille, M. Remy, S. Bellance, P. Chabassier, J.C. Fricain, J. Amedee, *Acta Biomater* **2010**, *6(7)*, 2494-2500. DOI: 10.1016/j.actbio.2009.09.029
[26] Y. Lin, Y. Huang, D.B. Chrisey, *Journal of Applied Physics* **2009**, *105(9)*. DOI: 10.1063/1.3116724
[27] P. Delaporte, A.-P. Alloncle, *Optics & Laser Technology* **2016**, *78(*33-41. DOI: 10.1016/j.optlastec.2015.09.022
[28] Z. Zhang, R. Xiong, R. Mei, Y. Huang, D.B. Chrisey, *Langmuir* **2015**, *31(23)*, 6447-6456. DOI: 10.1021/acs.langmuir.5b00919
[29] O. Kerouredan, J.M. Bourget, M. Remy, S. Crauste-Manciet, J. Kalisky, S. Catros, N.B. Thebaud, R. Devillard, *J Mater Sci Mater Med* **2019**, *30(2)*, 28. DOI: 10.1007/s10856-019-6230-1
[30] O. Kerouredan, D. Hakobyan, M. Remy, S. Ziane, N. Dusserre, J.C. Fricain, S. Delmond, N.B. Thebaud, R. Devillard, *Biofabrication* **2019**, *11(4)*, 045002. DOI: 10.1088/1758-5090/ab2620
[31] V. Keriquel, H. Oliveira, M. Remy, S. Ziane, S. Delmond, B. Rousseau, S. Rey, S. Catros, J. Amedee, F. Guillemot, J.C. Fricain, *Sci Rep* **2017**, *7(1)*, 1778. DOI: 10.1038/s41598-017-01914-x
[32] A. Ovsianikov, M. Gruene, M. Pflaum, L. Koch, F. Maiorana, M. Wilhelmi, A. Haverich, B. Chichkov, *Biofabrication* **2010**, *2(1)*, 014104. DOI: 10.1088/1758-5082/2/1/014104
[33] A. Palla-Papavlu, I. Paraico, J. Shaw-Stewart, V. Dinca, T. Savopol, E. Kovacs, T. Lippert, A. Wokaun, M. Dinescu, *Applied Physics A* **2010**, *102(3)*, 651-659. DOI: 10.1007/s00339-010-6114-1
[34] P. Serra, M. Colina, J.M. Fernández-Pradas, L. Sevilla, J.L. Morenza, *Applied Physics Letters* **2004**, *85(9)*, 1639-1641. DOI: 10.1063/1.1787614
[35] I. Zergioti, A. Karaiskou, D.G. Papazoglou, C. Fotakis, M. Kapsetaki, D. Kafetzopoulos, *Applied Surface Science* **2005**, *247(1-4)*, 584-589. DOI: 10.1016/j.apsusc.2005.01.127
[36] I. Zergioti, A. Karaiskou, D.G. Papazoglou, C. Fotakis, M. Kapsetaki, D. Kafetzopoulos, *Applied Physics Letters* **2005**, *86(16)*. DOI: 10.1063/1.1906325

This article is protected by copyright. All rights reserved.

Author Manuscript

21969744, 2021, 5, Downloaded from https://onlinelibrary.wiley.com/doi/10.1002/cben.202000037 by The University Of Texas Rio Grande Valley, Wiley Online Library on [13/12/2022]. See the Terms and Conditions (https://onlinelibrary.wiley.com/terms-and-conditions) on Wiley Online Library for rules of use; OA articles are governed by the applicable Creative Commons License

[37] M. Colina, P. Serra, J.M. Fernandez-Pradas, L. Sevilla, J.L. Morenza, *Biosens Bioelectron* **2005**, *20(8)*, 1638-1642. DOI: 10.1016/j.bios.2004.08.047
[38] J.A. Barron, H.D. Young, D.D. Dlott, M.M. Darfler, D.B. Krizman, B.R. Ringeisen, *Proteomics* **2005**, *5(16)*, 4138-4144. DOI: 10.1002/pmic.200401294
[39] S. Catros, J.C. Fricain, B. Guillotin, B. Pippenger, R. Bareille, M. Remy, E. Lebraud, B. Desbat, J. Amedee, F. Guillemot, *Biofabrication* **2011**, *3(2)*, 025001. DOI: 10.1088/1758-5082/3/2/025001
[40] F. Kawecki, W.P. Clafshenkel, F.A. Auger, J.M. Bourget, J. Fradette, R. Devillard, *Biofabrication* **2018**, *10(3)*, 035006. DOI: 10.1088/1758-5090/aabd5b
[41] S. Michael, H. Sorg, C.T. Peck, L. Koch, A. Deiwick, B. Chichkov, P.M. Vogt, K. Reimers, *PLoS One* **2013**, *8(3)*, e57741. DOI: 10.1371/journal.pone.0057741
[42] L. Koch, A. Deiwick, S. Schlie, S. Michael, M. Gruene, V. Coger, D. Zychlinski, A. Schambach, K. Reimers, P.M. Vogt, B. Chichkov, *Biotechnol Bioeng* **2012**, *109(7)*, 1855-1863. DOI: 10.1002/bit.24455
[43] B. Hopp, T. Smausz, Z. Antal, N. Kresz, Z. Bor, D. Chrisey, *Journal of applied physics* **2004**, *96(6)*, 3478-3481.
[44] J.M. Bourget, O. Kerouredan, M. Medina, M. Remy, N.B. Thebaud, R. Bareille, O. Chassande, J. Amedee, S. Catros, R. Devillard, *Biomed Res Int* **2016**, *2016(*3569843. DOI: 10.1155/2016/3569843
[45] M. Ali, E. Pages, A. Ducom, A. Fontaine, F. Guillemot, *Biofabrication* **2014**, *6(4)*, 045001. DOI: 10.1088/1758-5082/6/4/045001
[46] Y. Lin, D. Bourell, G. Huang, Y. Huang, T.R. Jeremy Tzeng, D. Chrisey, *Rapid Prototyping Journal* **2010**, *16(3)*, 202-208. DOI: 10.1108/13552541011034870
[47] A. Bakhshinejad, R.M.D. souza, A brief comparison between available bio-printing methods, 2015 IEEE Great Lakes Biomedical Conference (GLBC), 2015, pp. 1-3.
[48] L. Koch, A. Deiwick, A. Franke, K. Schwanke, A. Haverich, R. Zweigerdt, B. Chichkov, *Biofabrication* **2018**, *10(3)*, 035005. DOI: 10.1088/1758-5090/aab981
[49] B.R. Ringeisen, K. Rincon, L.A. Fitzgerald, P.A. Fulmer, P.K. Wu, M. Gilbert, *Methods in Ecology and Evolution* **2014**, *6(2)*, 209-217. DOI: 10.1111/2041-210x.12303
[50] M.S. Brown, N.T. Kattamis, C.B. Arnold, *Journal of Applied Physics* **2010**, *107(8)*, 083103. DOI: 10.1063/1.3327432
[51] P. Serra, M. Duocastella, J.M. Fernández-Pradas, J.L. Morenza, *Applied Surface Science* **2009**, *255(10)*, 5342-5345. DOI: 10.1016/j.apsusc.2008.07.200
[52] M. Gruene, A. Deiwick, L. Koch, S. Schlie, C. Unger, N. Hofmann, I. Bernemann, B. Glasmacher, B. Chichkov, *Tissue Eng Part C Methods* **2011**, *17(1)*, 79-87. DOI: 10.1089/ten.TEC.2010.0359
[53] J.M. Fernández-Pradas, Á. Rodríguez-Vázquez, M. Duocastella, M. Colina, G. Liñán-Cembrano, P. Serra, J.L. Morenza, Production of miniaturized biosensors through laser-induced forward transfer, Bioengineered and Bioinspired Systems III, 2007.
[54] A.K. Nguyen, R.J. Narayan, *Ann Biomed Eng* **2017**, *45(1)*, 84-99. DOI: 10.1007/s10439-016-1617-3
[55] C.M. Othon, X. Wu, J.J. Anders, B.R. Ringeisen, *Biomed Mater* **2008**, *3(3)*, 034101. DOI: 10.1088/1748-6041/3/3/034101
[56] C.Y. Chen, J.A. Barron, B.R. Ringeisen, *Applied Surface Science* **2006**, *252(24)*, 8641-8645. DOI: 10.1016/j.apsusc.2005.11.088
[57] A. Karaiskou, I. Zergioti, C. Fotakis, M. Kapsetaki, D. Kafetzopoulos, *Applied Surface Science* **2003**, *208-209(*245-249. DOI: 10.1016/s0169-4332(02)01396-x
[58] M. Duocastella, J.M. Fernández-Pradas, J.L. Morenza, D. Zafra, P. Serra, *Sensors and Actuators B: Chemical* **2010**, *145(1)*, 596-600. DOI: 10.1016/j.snb.2009.11.055
[59] V. Dinca, M. Farsari, D. Kafetzopoulos, A. Popescu, M. Dinescu, C. Fotakis, *Thin Solid Films* **2008**, *516(18)*, 6504-6511. DOI: 10.1016/j.tsf.2008.02.043
[60] B. Hopp, T. Smausz, A. Nógrádi, Absorbing-Film Assisted Laser Induced Forward Transfer of Sensitive Biological Subjects, in: B.R. Ringeisen, B.J. Spargo, P.K. Wu (Eds.), Cell and Organ Printing, Springer Netherlands, Dordrecht, 2010, pp. 115-134.
[61] E. Pagès, M. Rémy, V. Kériquel, M.M. Correa, B. Guillotin, F. Guillemot, *Journal of Nanotechnology in Engineering and Medicine* **2015**, *6(2)*. DOI: 10.1115/1.4031217
[62] V. Yusupov, S. Churbanov, E. Churbanova, K. Bardakova, A. Antoshin, S. Evlashin, P. Timashev, N. Minaev, *International journal of bioprinting* **2020**, *6(3)*, 271-271. DOI: 10.18063/ijb.v6i3.271
[63] J. Zhang, B. Hartmann, J. Siegel, G. Marchi, H. Clausen-Schaumann, S. Sudhop, H.P. Huber, *PLoS One* **2018**, *13(5)*, e0195479. DOI: 10.1371/journal.pone.0195479
[64] P. Serra, M. Duocastella, J.M. Fernández-Pradas, J.L. Morenza, Laser-Induced Forward Transfer: A Laser-Based Technique for Biomolecules Printing, Cell and Organ Printing2010, pp. 53-80.

This article is protected by copyright. All rights reserved.

Author Manuscript

21969744, 2021, 5, Downloaded from https://onlinelibrary.wiley.com/doi/10.1002/cben.202000037 by The University Of Texas Rio Grande Valley, Wiley Online Library on [13/12/2022]. See the Terms and Conditions (https://onlinelibrary.wiley.com/terms-and-conditions) on Wiley Online Library for rules of use; OA articles are governed by the applicable Creative Commons License

[65] J.A. Barron, B.R. Ringeisen, H. Kim, B.J. Spargo, D.B. Chrisey, *Thin Solid Films* **2004**, *453-454(*383-387. DOI: 10.1016/j.tsf.2003.11.161
[66] M. Duocastella, J.M. Fernández-Pradas, J.L.M.P. Serra, *Thin Solid Films* **2010**, *518(18)*, 5321-5325. DOI: 10.1016/j.tsf.2010.03.082
[67] M. Duocastella, J.M. Fernández-Pradas, J.L. Morenza, P. Serra, *Journal of applied physics* **2009**, *106(8)*, 084907. DOI: 10.1063/1.3248304
[68] C. Unger, M. Gruene, L. Koch, J. Koch, B.N. Chichkov, *Applied Physics A* **2010**, *103(2)*, 271-277. DOI: 10.1007/s00339-010-6030-4
[69] M. Duocastella, J.M. Fernández-Pradas, P. Serra, J.L. Morenza, *Applied Physics A* **2008**, *93(2)*, 453-456. DOI: 10.1007/s00339-008-4781-y
[70] F. Guillemot, A. Souquet, S. Catros, B. Guillotin, *Nanomedicine* **2010**, *5(3)*, 507-515.
[71] M. Duocastella, A. Patrascioiu, J.M. Fernández-Pradas, J.L. Morenza, P. Serra, *Opt. Express* **2010**, *18(21)*, 21815-21825. DOI: 10.1364/OE.18.021815
[72] B. Hopp, T. Smausz, N. Kresz, N. Barna, Z. Bor, L. Kolozsvári, D.B. Chrisey, A. Szabó, A. Nógrádi, *Tissue Engineering* **2005**, *11(11-12)*, 1817-1823. DOI: 10.1089/ten.2005.11.1817
[73] A. Doraiswamy, R.J. Narayan, T. Lippert, L. Urech, A. Wokaun, M. Nagel, B. Hopp, M. Dinescu, R. Modi, R.C.Y. Auyeung, D.B. Chrisey, *Applied Surface Science* **2006**, *252(13)*, 4743-4747. DOI: 10.1016/j.apsusc.2005.07.166
[74] T. Smausz, B. Hopp, G. Kecskeméti, Z. Bor, *Applied Surface Science* **2006**, *252(13)*, 4738-4742. DOI: 10.1016/j.apsusc.2005.07.115
[75] C. Boutopoulos, I. Kalpyris, E. Serpetzoglou, I. Zergioti, *Microfluidics and Nanofluidics* **2013**, *16(3)*, 493-500. DOI: 10.1007/s10404-013-1248-z
[76] Y. Deng, P. Renaud, Z. Guo, Z. Huang, Y. Chen, *J Biol Eng* **2017**, *11(*2. DOI: 10.1186/s13036-016-0045-0
[77] Y. Lin, Y. Huang, D.B. Chrisey, *Journal of Biomechanical Engineering* **2011**, *133(2)*. DOI: 10.1115/1.4003132
[78] V.I. Yusupov, V.S. Zhigar'kov, E.S. Churbanova, E.A. Chutko, S.A. Evlashin, M.V. Gorlenko, V.S. Cheptsov, N.V. Minaev, V.N. Bagratashvili, *Quantum Electronics* **2017**, *47(12)*, 1158-1165. DOI: 10.1070/qel16512
[79] M. Colina, M. Duocastella, J.M. Fernández-Pradas, P. Serra, J.L. Morenza, *Journal of Applied Physics* **2006**, *99(8)*. DOI: 10.1063/1.2191569
[80] L. Koch, A. Deiwick, B. Chichkov, *BioNanoMaterials* **2014**, *15(3-4)*. DOI: 10.1515/bnm-2014-0005
[81] A.J. Haider, M.J. Haider, M.D. Majed, A.H. Mohammed, H.L. Mansour, *Energy Procedia* **2017**, *119(*256-263. DOI: https://doi.org/10.1016/j.egypro.2017.07.078
[82] P. Serra, A. Piqué, *Advanced Materials Technologies* **2019**, *4(1)*. DOI: 10.1002/admt.201800099
[83] R. Xiong, Z. Zhang, W. Chai, D.B. Chrisey, Y. Huang, *Biofabrication* **2017**, *9(2)*, 024103. DOI: 10.1088/1758-5090/aa74f2
[84] K.M. Charipar, R.E. Diaz-Rivera, N.H. De Jesus-Villanueva, R.C.Y. Auyeung, N.A. Charipar, A. Piqué, G. Račiukaitis, T. Makimura, C. Molpeceres, Reusable laser-absorbing layers for LIFT, Laser Applications in Microelectronic and Optoelectronic Manufacturing (LAMOM) XXIV, 2019.
[85] J. Yan, Y. Huang, D.B. Chrisey, *Biofabrication* **2013**, *5(1)*, 015002. DOI: 10.1088/1758-5082/5/1/015002
[86] H. Gudapati, J. Yan, Y. Huang, D.B. Chrisey, *Biofabrication* **2014**, *6(3)*, 035022. DOI: 10.1088/1758-5082/6/3/035022
[87] B. Guillotin, M. Ali, A. Ducom, S. Catros, V. Keriquel, A. Souquet, M. Remy, J.-C. Fricain, F. Guillemot, Laser-Assisted Bioprinting for Tissue Engineering, Biofabrication2013, pp. 95-118.
[88] M. Duocastella, M. Colina, J.M. Fernández-Pradas, P. Serra, J.L. Morenza, *Applied Surface Science* **2007**, *253(19)*, 7855-7859. DOI: 10.1016/j.apsusc.2007.02.097
[89] M. Duocastella, J.M. Fernández-Pradas, J. Domínguez, P. Serra, J.L. Morenza, *Applied Physics A* **2008**, *93(4)*, 941-945. DOI: 10.1007/s00339-008-4741-6
[90] J. Yan, Y. Huang, C. Xu, D.B. Chrisey, *Journal of Applied Physics* **2012**, *112(8)*. DOI: 10.1063/1.4759344
[91] M. Gruene, C. Unger, L. Koch, A. Deiwick, B. Chichkov, *BioMedical Engineering OnLine* **2011**, *10(1)*, 19. DOI: 10.1186/1475-925X-10-19
[92] Z. Zhang, R. Xiong, D.T. Corr, Y. Huang, *Langmuir* **2016**, *32(12)*, 3004-3014. DOI: 10.1021/acs.langmuir.6b00220
[93] Z. Zhang, C. Xu, R. Xiong, D.B. Chrisey, Y. Huang, *Biomicrofluidics* **2017**, *11(3)*, 034120. DOI: 10.1063/1.4985652

This article is protected by copyright. All rights reserved.

Author Manuscript

21969744, 2021, 5, Downloaded from https://onlinelibrary.wiley.com/doi/10.1002/cben.202000037 by The University Of Texas Rio Grande Valley, Wiley Online Library on [13/12/2022]. See the Terms and Conditions (https://onlinelibrary.wiley.com/terms-and-conditions) on Wiley Online Library for rules of use; OA articles are governed by the applicable Creative Commons License

[94] L. Ouyang, R. Yao, Y. Zhao, W. Sun, *Biofabrication* **2016**, *8(3)*, 035020. DOI: 10.1088/1758-5090/8/3/035020
[95] J. Qu, C. Dou, J. Li, Z. Rao, B. Xu, Numerical and Experimental Study of Bioink Transfer Process in Laser Induced Forward Transfer (LIFT) 3D Bioprinting, ASME 2020 Heat Transfer Summer Conference collocated with the ASME 2020 Fluids Engineering Division Summer Meeting and the ASME 2020 18th International Conference on Nanochannels, Microchannels, and Minichannels, 2020.
[96] V. Mironov, T. Trusk, V. Kasyanov, S. Little, R. Swaja, R. Markwald, *Biofabrication* **2009**, *1(2)*, 022001. DOI: 10.1088/1758-5082/1/2/022001
[97] P.S. Hoppe, D.L. Coutu, T. Schroeder, *Nat Cell Biol* **2014**, *16(10)*, 919-927. DOI: 10.1038/ncb3042
[98] J. Riba, N. Renz, C. Niemoller, S. Bleul, D. Pfeifer, J.M. Stosch, K.H. Metzeler, B. Hackanson, M. Lubbert, J. Duyster, P. Koltay, R. Zengerle, R. Claus, S. Zimmermann, H. Becker, *PLoS One* **2016**, *11(9)*, e0163455. DOI: 10.1371/journal.pone.0163455
[99] A. Gross, J. Schoendube, S. Zimmermann, M. Steeb, R. Zengerle, P. Koltay, *Int J Mol Sci* **2015**, *16(8)*, 16897-16919. DOI: 10.3390/ijms160816897
[100] P. Hu, W. Zhang, H. Xin, G. Deng, *Front Cell Dev Biol* **2016**, *4(*116. DOI: 10.3389/fcell.2016.00116
[101] A.R. Liberski, J.T. Delaney, Jr., U.S. Schubert, *ACS Comb Sci* **2011**, *13(2)*, 190-195. DOI: 10.1021/co100061c
[102] B.C. Riggs, A.D. Dias, N.R. Schiele, R. Cristescu, Y. Huang, D.T. Corr, D.B. Chrisey, *MRS Bulletin* **2011**, *36(12)*, 1043-1050. DOI: 10.1557/mrs.2011.276
[103] J.A. Barron, D.B. Krizman, B.R. Ringeisen, *Ann Biomed Eng* **2005**, *33(2)*, 121-130. DOI: 10.1007/s10439-005-8971-x
[104] A. Márquez, M. Gómez-Fontela, S. Lauzurica, R. Candorcio-Simon, D. Munoz-Martin, M. Morales, M. Ubago, C. Toledo, P. Lauzurica, C. Molpeceres, *Biofabrication* **2020**, *12(2)*, 025019.
[105] W. Wang, G. Li, Y. Huang, *Journal of Manufacturing Science and Engineering* **2009**, *131(5)*. DOI: 10.1115/1.4000101
[106] R. Xiong, Z. Zhang, J. Shen, Y. Lin, Y. Huang, D.B. Chrisey, *Journal of Micro and Nano-Manufacturing* **2015**, *3(1)*. DOI: 10.1115/1.4029264
[107] C. Mezel, A. Souquet, L. Hallo, F. Guillemot, *Biofabrication* **2010**, *2(1)*, 014103. DOI: 10.1088/1758-5082/2/1/014103
[108] P.K. Kennedy, S.A. Boppart, D.X. Hammer, B.A. Rockwell, G.D. Noojin, W.P. Roach, *IEEE Journal of Quantum Electronics* **1995**, *31(12)*, 2250-2257. DOI: 10.1109/3.477754
[109] A. Vogel, J. Noack, K. Nahen, D. Theisen, S. Busch, U. Parlitz, D.X. Hammer, G.D. Noojin, B.A. Rockwell, R. Birngruber, *Applied Physics B* **1999**, *68(2)*, 271-280. DOI: 10.1007/s003400050617
[110] F. Pati, J. Jang, D.H. Ha, S. Won Kim, J.W. Rhie, J.H. Shim, D.H. Kim, D.W. Cho, *Nat Commun* **2014**, *5(*3935. DOI: 10.1038/ncomms4935
[111] R. Xiong, Z. Zhang, W. Chai, Y. Huang, D.B. Chrisey, *Biofabrication* **2015**, *7(4)*, 045011. DOI: 10.1088/1758-5090/7/4/045011
[112] S. Catros, B. Guillotin, M. Bačáková, J.-C. Fricain, F. Guillemot, *Applied Surface Science* **2011**, *257(12)*, 5142-5147. DOI: 10.1016/j.apsusc.2010.11.049
[113] X. Cui, D. Dean, Z.M. Ruggeri, T. Boland, *Biotechnol Bioeng* **2010**, *106(6)*, 963-969. DOI: 10.1002/bit.22762
[114] Z. Zhang, W. Chai, R. Xiong, L. Zhou, Y. Huang, *Biofabrication* **2017**, *9(2)*, 025038. DOI: 10.1088/1758-5090/aa6ed9
[115] J. Zhang, P. Byers, C. Frank, L. Schulte-Spechtel, B. Hartmann, J. Siegel, G. Marchi, D. Docheva, H. Clausen-Schaumann, S. Sudhop, H.P. Huber, Femtosecond laser printing of living human cells, Clinical and Preclinical Optical Diagnostics II, Optical Society of America, Munich, 2019, p. 11079_11035.
[116] B.R. Ringeisen, H. Kim, J.A. Barron, D.B. Krizman, D.B. Chrisey, S. Jackman, R.Y.C. Auyeung, B.J. Spargo, *Tissue Engineering* **2004**, *10(3-4)*, 483-491. DOI: 10.1089/107632704323061843
[117] L. Koch, S. Kuhn, H. Sorg, M. Gruene, S. Schlie, R. Gaebel, B. Polchow, K. Reimers, S. Stoelting, N. Ma, P.M. Vogt, G. Steinhoff, B. Chichkov, *Tissue Eng Part C Methods* **2010**, *16(5)*, 847-854. DOI: 10.1089/ten.TEC.2009.0397
[118] L. Koch, M. Gruene, C. Unger, B. Chichkov, *Current Pharmaceutical Biotechnology* **2013**, *14(1)*, 91-97. DOI: 10.2174/138920113804805368
[119] W. Wang, Y. Lin, Y. Huang, *Journal of Manufacturing Science and Engineering* **2011**, *133(2)*. DOI: 10.1115/1.4003612
[120] T. Xu, J. Rohozinski, W. Zhao, E.C. Moorefield, A. Atala, J.J. Yoo, *Tissue Engineering Part A* **2009**, *15(1)*, 95-101.
[121] S. Stolberg, K.E. McCloskey, *Biotechnology Progress* **2009**, *25(1)*, 10-19. DOI: 10.1002/btpr.124

This article is protected by copyright. All rights reserved.

Author Manuscript

21969744, 2021, 5, Downloaded from https://onlinelibrary.wiley.com/doi/10.1002/cben.202000037 by The University Of Texas Rio Grande Valley, Wiley Online Library on [13/12/2022]. See the Terms and Conditions (https://onlinelibrary.wiley.com/terms-and-conditions) on Wiley Online Library for rules of use; OA articles are governed by the applicable Creative Commons License

[122] Y. Lin, Y. Huang, G. Wang, T.-R.J. Tzeng, D.B. Chrisey, *Journal of Applied Physics* **2009**, *106(4)*. DOI: 10.1063/1.3202388
[123] D. Riester, *Journal of Laser Micro/Nanoengineering* **2016**, *11(2)*, 199-203. DOI: 10.2961/jlmn.2016.02.0010
[124] M. Akerfelt, R.I. Morimoto, L. Sistonen, *Nat Rev Mol Cell Biol* **2010**, *11(8)*, 545-555. DOI: 10.1038/nrm2938
[125] K. Miazek, W. Iwanek, C. Remacle, A. Richel, D. Goffin, *Int J Mol Sci* **2015**, *16(10)*, 23929-23969. DOI: 10.3390/ijms161023929
[126] Z. Chen, J. Lu, S.H. Gao, M. Jin, P.L. Bond, P. Yang, Z. Yuan, J. Guo, *Water Res* **2018**, *129(*163-171. DOI: 10.1016/j.watres.2017.11.021
[127] P.V. Asharani, M.P. Hande, S. Valiyaveettil, *BMC Cell Biol* **2009**, *10(*65. DOI: 10.1186/1471-2121-10-65

Author Manuscript

This article is protected by copyright. All rights reserved.

21969744, 2021, 5, Downloaded from https://onlinelibrary.wiley.com/doi/10.1002/cben.202000037 by The University Of Texas Rio Grande Valley, Wiley Online Library on [13/12/2022]. See the Terms and Conditions (https://onlinelibrary.wiley.com/terms-and-conditions) on Wiley Online Library for rules of use; OA articles are governed by the applicable Creative Commons License

Figures

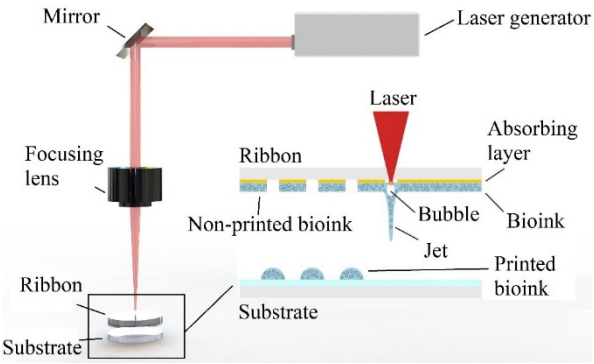

Figure 1. Structure and main components of a laser-assisted bioprinter (modified from [48]).

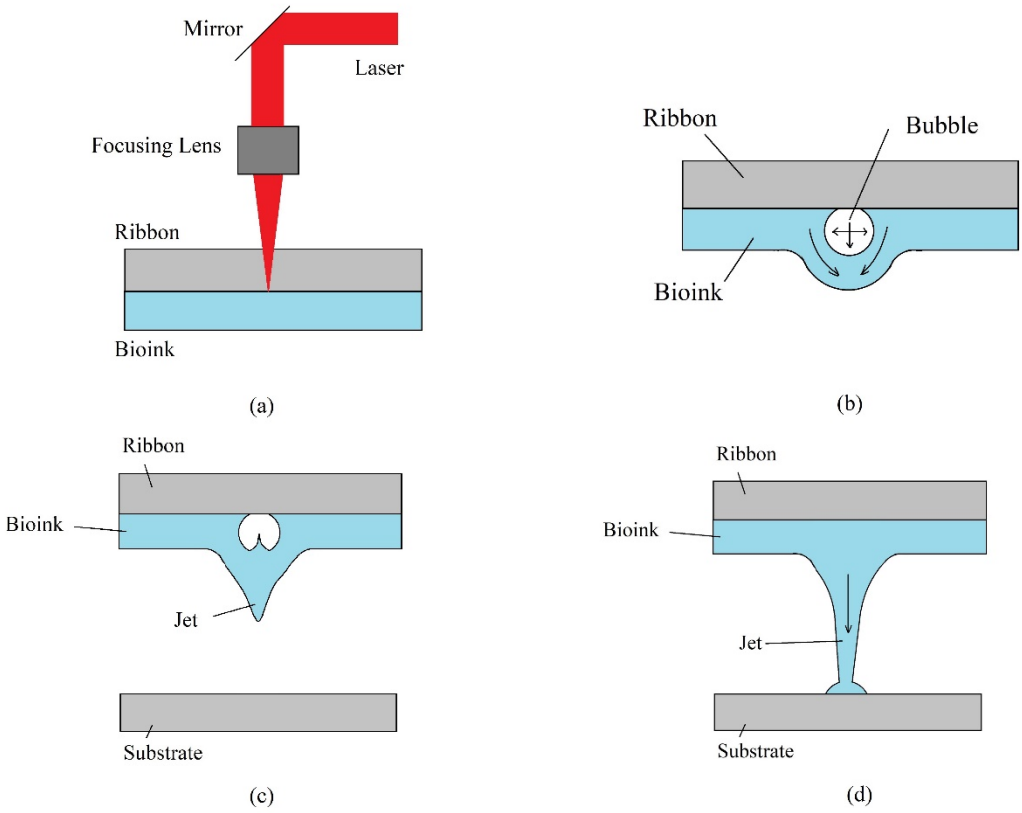

Figure 2. LAB working process: (a) step 1; (b) step 2; (c) step 3; (d) step 4.

This article is protected by copyright. All rights reserved.

21969744, 2021, 5, Downloaded from https://onlinelibrary.wiley.com/doi/10.1002/cben.202000037 by The University Of Texas Rio Grande Valley, Wiley Online Library on [13/12/2022]. See the Terms and Conditions (https://onlinelibrary.wiley.com/terms-and-conditions) on Wiley Online Library for rules of use; OA articles are governed by the applicable Creative Commons License

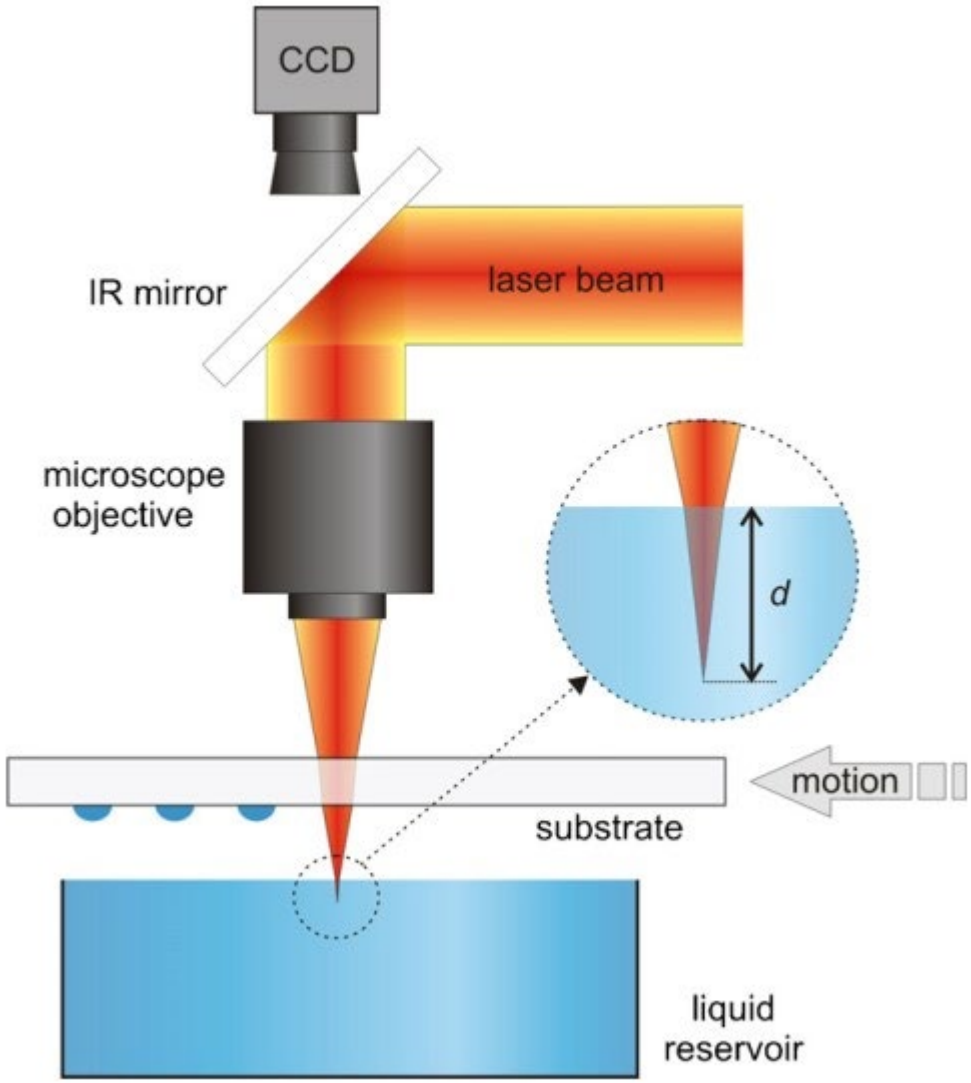

Figure 3. Laser-induced backward transfer [58].

This article is protected by copyright. All rights reserved.

21969744, 2021, 5, Downloaded from https://onlinelibrary.wiley.com/doi/10.1002/cben.202000037 by The University Of Texas Rio Grande Valley, Wiley Online Library on [13/12/2022]. See the Terms and Conditions (https://onlinelibrary.wiley.com/terms-and-conditions) on Wiley Online Library for rules of use; OA articles are governed by the applicable Creative Commons License

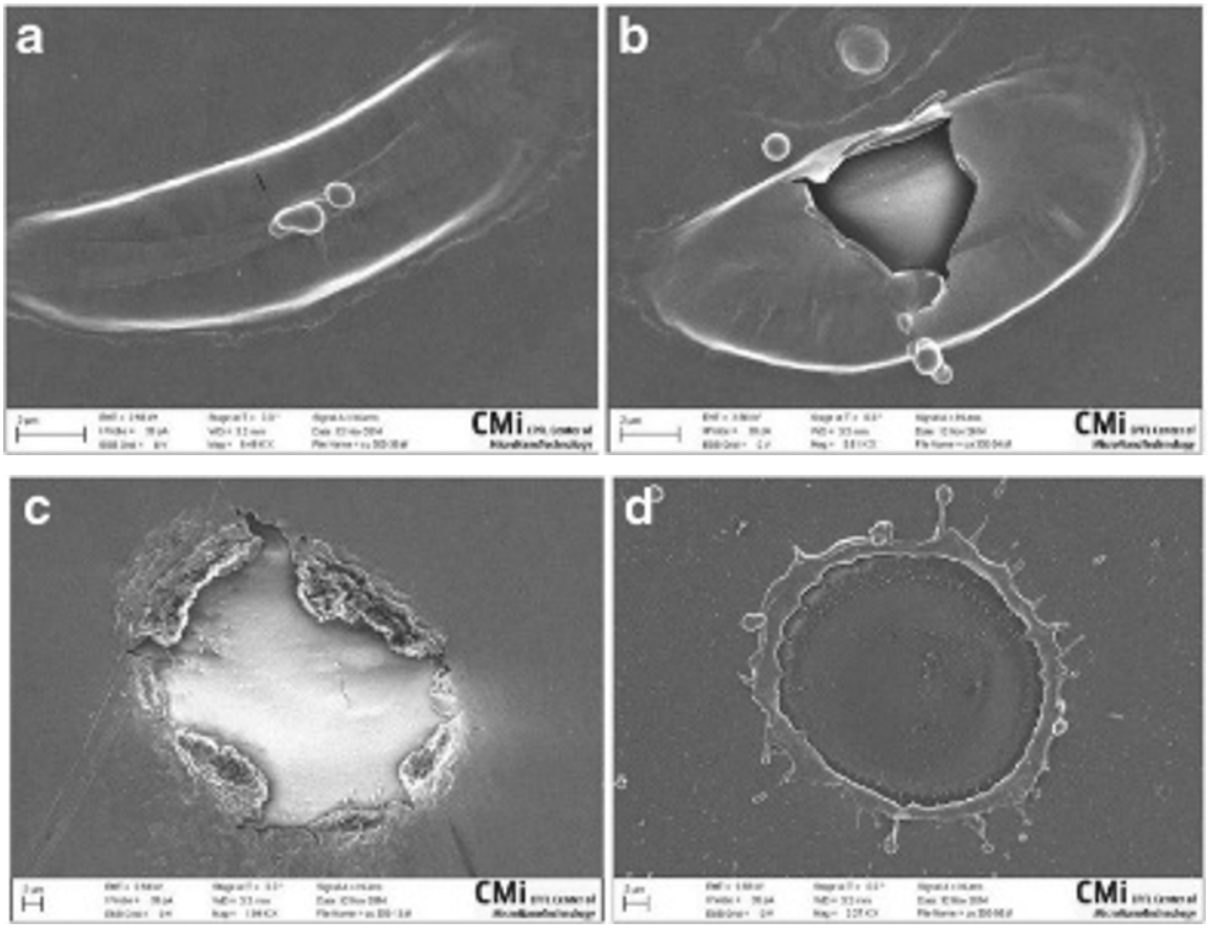

Figure 4. Morphologies of EAL (titanium) after LAB. (a) Pulse energy 2 μJ, spot size 45 μm, thickness 160 nm; (b) pulse energy 2 μJ, spot size 45 μm, thickness 100 nm; (c) pulse energy 2 μJ, spot size 45 μm, thickness 80 nm; (d) pulse energy 2 μJ, spot size 45 μm, thickness 40 nm [76].

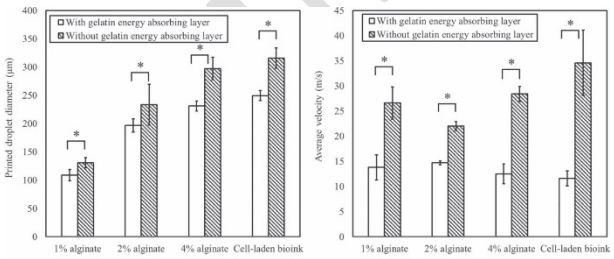

Figure 5. (a) Droplet size and (b) jet velocity with/without the gelatin EAL; * indicates significant difference between groups [83].

This article is protected by copyright. All rights reserved.

21969744, 2021, 5, Downloaded from https://onlinelibrary.wiley.com/doi/10.1002/cben.202000037 by The University Of Texas Rio Grande Valley, Wiley Online Library on [13/12/2022]. See the Terms and Conditions (https://onlinelibrary.wiley.com/terms-and-conditions) on Wiley Online Library for rules of use; OA articles are governed by the applicable Creative Commons License

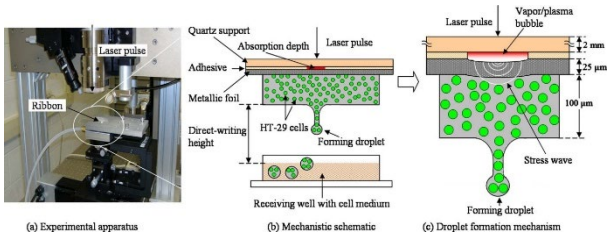

Figure 6. Metallic foil-assisted laser cell transfer [77].

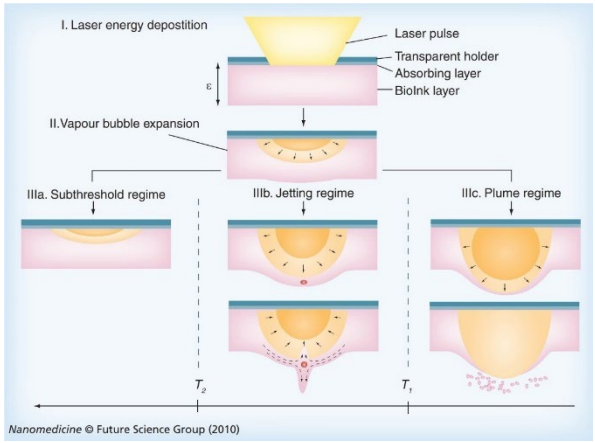

Figure 7. Three regimes for bubble/jet formation [70].

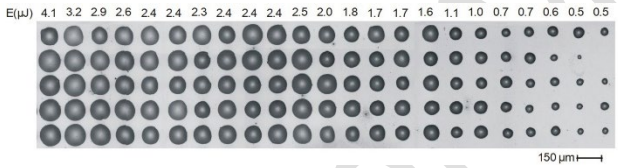

Figure 8. Droplets transferred at different laser energies; over each column, the average pulse energy is indicated [53].

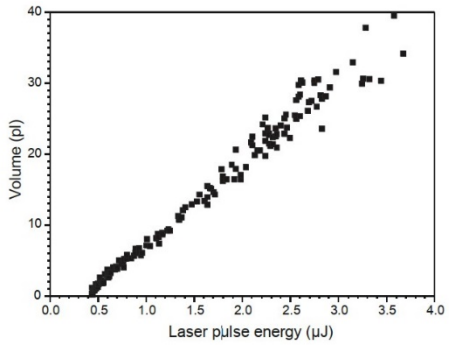

Figure 9. Droplet volume versus laser pulse energy [53].

This article is protected by copyright. All rights reserved.

21969744, 2021, 5, Downloaded from https://onlinelibrary.wiley.com/doi/10.1002/cben.202000037 by The University Of Texas Rio Grande Valley, Wiley Online Library on [13/12/2022]. See the Terms and Conditions (https://onlinelibrary.wiley.com/terms-and-conditions) on Wiley Online Library for rules of use; OA articles are governed by the applicable Creative Commons License

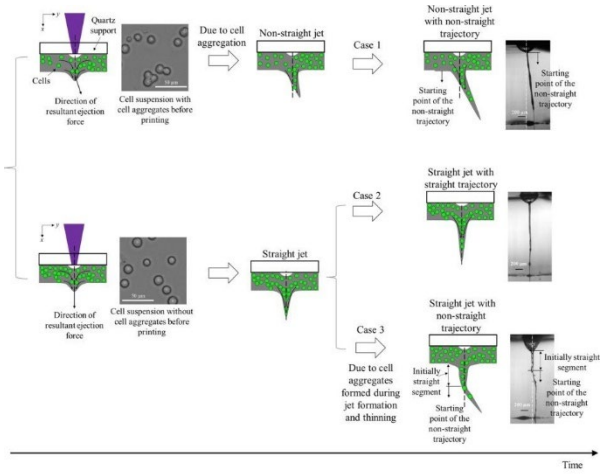

Figure 10. Different types of jets by using the cell-laden bioink [93].

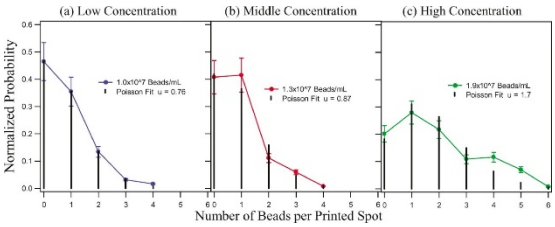

Figure 11. Number of beads printed every time with concentrations of 1.0, 1.3, and 1.9×10^7 beads mL^{-1} [103].

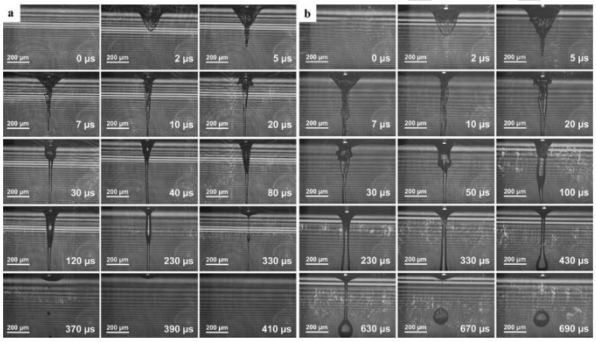

Figure 12. Time-resolved images of the jet formation during LAB. Laser power: (a) 1.6 J cm^{-2}; (b) 2.7 J cm^{-2} [68].

This article is protected by copyright. All rights reserved.

21969744, 2021, 5, Downloaded from https://onlinelibrary.wiley.com/doi/10.1002/cben.202000037 by The University Of Texas Rio Grande Valley, Wiley Online Library on [13/12/2022]. See the Terms and Conditions (https://onlinelibrary.wiley.com/terms-and-conditions) on Wiley Online Library for rules of use; OA articles are governed by the applicable Creative Commons License

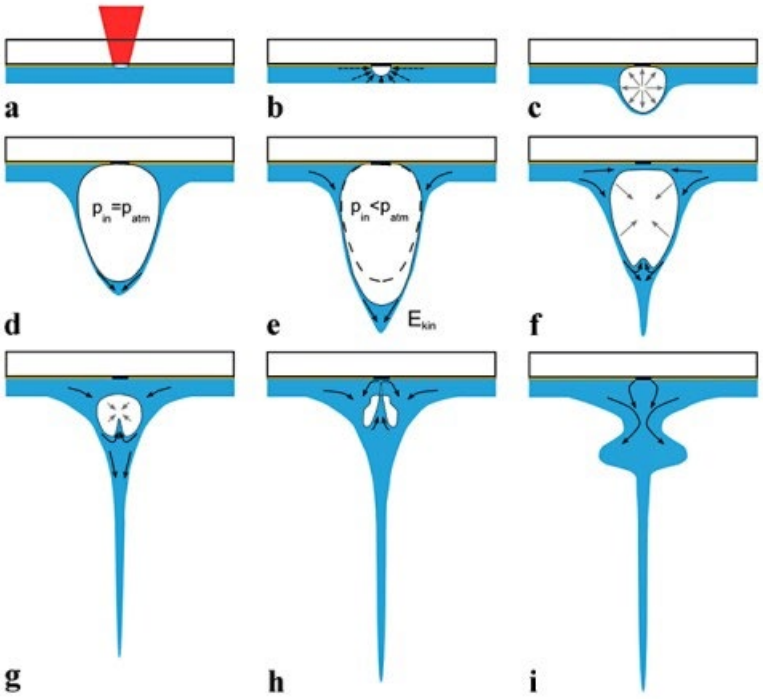

Figure 13. Bubble/jet formation process of LAB [68].

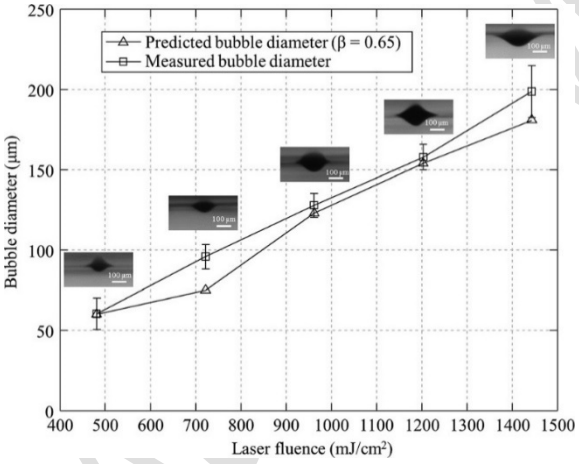

Figure 14. Transferred droplet volume versus laser pulse energy [106].

This article is protected by copyright. All rights reserved.

21969744, 2021, 5, Downloaded from https://onlinelibrary.wiley.com/doi/10.1002/cben.202000037 by The University Of Texas Rio Grande Valley, Wiley Online Library on [13/12/2022]. See the Terms and Conditions (https://onlinelibrary.wiley.com/terms-and-conditions) on Wiley Online Library for rules of use; OA articles are governed by the applicable Creative Commons License

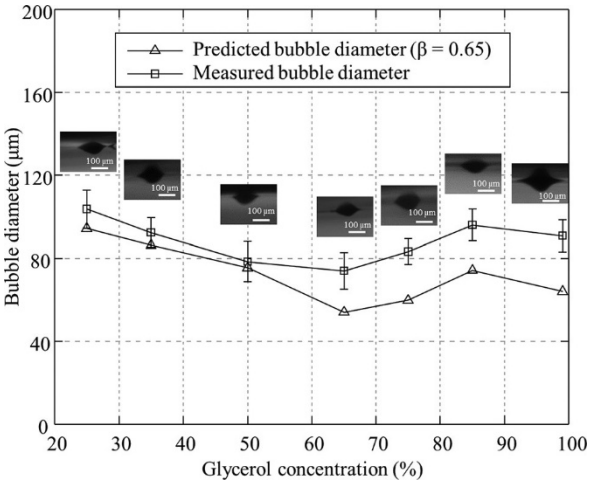

Figure 15. Maximum bubble diameter under a 722 mJ cm^{-2} laser fluence [106].

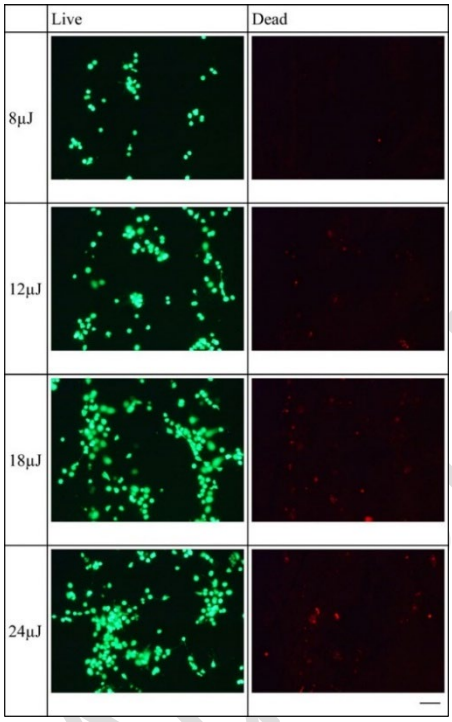

Figure 16. Effect of laser energy on cell viability (bar = 100 μm) [112].

This article is protected by copyright. All rights reserved.

21969744, 2021, 5, Downloaded from https://onlinelibrary.wiley.com/doi/10.1002/cben.202000037 by The University Of Texas Rio Grande Valley, Wiley Online Library on [13/12/2022]. See the Terms and Conditions (https://onlinelibrary.wiley.com/terms-and-conditions) on Wiley Online Library for rules of use; OA articles are governed by the applicable Creative Commons License